



Article

Biodegradable Polyhydroxyalkanoates Formed by 3- and 4-Hydroxybutyrate Monomers to Produce Nanomembranes Suitable for Drug Delivery and Cell Culture

Tatiana G. Volova^{1,2}, Aleksey V. Demidenko^{1,2}, Anastasiya V. Murueva^{1,2,*}, Alexey E. Dudaev^{1,2}, Ivan Nemtsev^{2,3,4} and Ekaterina I. Shishatskaya^{1,2,5}

- ¹ Institute of Biophysics SB RAS, Federal Research Center “Krasnoyarsk Science Center SB RAS”, 50/50 Akademgorodok, 660036 Krasnoyarsk, Russia; volova45@mail.ru (T.G.V.); kraysolnca@mail.ru (A.V.D.); alex15-96@mail.ru (A.E.D.); shishatskaya@inbox.ru (E.I.S.)
- ² Institute of Fundamental Biology and Biotechnology, Siberian Federal University, 79 Svobodnyi av., 660041 Krasnoyarsk, Russia; ivan_nemtsev@mail.ru
- ³ Federal Research Center “Krasnoyarsk Science Center SB RAS”, 50 Akademgorodok, 660036 Krasnoyarsk, Russia
- ⁴ L.V. Kirensky Institute of Physics, 50/12 Akademgorodok, 660036 Krasnoyarsk, Russia
- ⁵ Chemistry Engineering Centre, ITMO University, Kronverkskiy Prospekt, 49A, 197101 Saint Petersburg, Russia
- * Correspondence: goreva_a@mail.ru

Abstract: Biodegradable polyhydroxyalkanoates, biopolymers of microbiological origin, formed by 3- and 4-hydroxybutyrate monomers P(3HB-co-4HB), were used to obtain nanomembranes loaded with drugs as cell carriers by electrospinning. Resorbable non-woven membranes from P(3HB-co-4HB) loaded with ceftazidime, doripinem, and actovegin have been obtained. The loading of membranes with drugs differently affected the size of fibers and the structure of membranes, and in all cases increased the hydrophilicity of the surface. The release of drugs in vitro was gradual, which corresponded to the Higuchi and Korsmeyer-Peppas models. Antibiotic-loaded membranes showed antibacterial activity against *S. aureus* and *E. coli*, in which growth inhibition zones were 41.7 ± 1.1 and 38.6 ± 1.7 mm for ceftazidime and doripinem, respectively. The study of the biological activity of membranes in the NIH 3T3 mouse fibroblast culture based on the results of DAPI and FITC staining of cells, as well as the MTT test, did not reveal a negative effect despite the presence of antibiotics in them. Samples containing actovegin exhibit a stimulating effect on fibroblasts. Biodegradable polyhydroxyalkanoates formed by 3-hydroxybutyrate and 4-hydroxybutyrate monomers provide electrospinning non-woven membranes suitable for long-term delivery of drugs and cultivation of eukaryotic cells, and are promising for the treatment of wound defects complicated by infection.

Keywords: degradable polyhydroxyalkanoates; copolymers P(3HB-co-4HB); electrostatic molding; membranes; microstructure and properties; drugs; release kinetics; antibacterial activity; fibroblast proliferation



Citation: Volova, T.G.; Demidenko, A.V.; Murueva, A.V.; Dudaev, A.E.; Nemtsev, I.; Shishatskaya, E.I. Biodegradable Polyhydroxyalkanoates Formed by 3- and 4-Hydroxybutyrate Monomers to Produce Nanomembranes Suitable for Drug Delivery and Cell Culture. *Technologies* **2023**, *11*, 106. <https://doi.org/10.3390/technologies11040106>

Academic Editor: Yury A. Skorik

Received: 19 July 2023

Revised: 3 August 2023

Accepted: 6 August 2023

Published: 7 August 2023



Copyright: © 2023 by the authors. Licensee MDPI, Basel, Switzerland. This article is an open access article distributed under the terms and conditions of the Creative Commons Attribution (CC BY) license (<https://creativecommons.org/licenses/by/4.0/>).

1. Introduction

Polyhydroxyalkanoates are biodegradable polymers of microbiological origin, have a high biomedical potential and are suitable for obtaining products by various methods, including modern additive technologies and electrospinning [1,2]. Electrostatic molding (ESM), or electrostatic formation (ESF)—“electrospinning”—is one of the most promising methods for obtaining materials and products for biomedicine. By the nature of the technological process, electrospinning is a spinnerless method in which the polymer solution is drawn out, the resulting fibers are cured, and the non-woven fibrous layer is formed using electrical voltage in a single working space [3,4]. The principle of the method is based on the formation of ultrathin elongated structures in an electrostatic field formed between oppositely charged electrodes; when one of them is in a melt or solution of a polymer

material, the second is placed on a receiving metal collector (target). The simplicity of hardware production of electrostatic spinning, high efficiency, versatility in the choice of polymeric materials, and a wide range of control parameters have made the ESF method attractive not only for laboratory, but also for industrial production of nanofibers [5,6]. Industrial scale ESF allows to obtain non-woven materials of various sizes [7].

The ESF method makes it possible to obtain ultra- and nano-thin fibers and porous non-woven nanomembranes from solutions and melts of polymers of various structures, which are used in medicine, bioengineering, electronics, for filtering gases and liquids, in the creation of composite materials, etc. [8,9]. The ESF method has been strongly developed in recent years due to the needs of new biomedical technologies, in particular, cell and tissue engineering, which are in dire need of functional scaffolds. The ESF technology allows for systems that are as close as possible to the characteristics of native tissues [3] from materials of various origins, including natural and synthetic polymers, such as collagen, fibrinogen, silk, chitosan, gelatin, carboxymethyl cellulose, polycaprolactone, polylactide, polyurethanes, polyvinyl alcohol, polyethylene oxide, and others [3,10–15]. Non-woven nanomaterials based on ultrathin fibers serve not only as a substrate (matrix) for growing cells, but can also be used as drug carriers [16]. The use of such systems is especially important for the local treatment of damaged areas of organs and tissues, including the protection and treatment of damaged tissues in the postoperative period. Thus, areas in particular need for functional nanomaterials obtained by the ESF method are cell and tissue engineering associated with the restoration of damaged organs and tissues, and the creation of long-term and controlled systems for the deposition and delivery of drugs.

Using the ESF method, non-woven fibers with prolonged release of drugs based on polyethylene oxide, polyvinylpyrrolidone, poly-(lactic acid) and poly-(butylene adipate)-co-(butylene terephthalate), cellulose acetate, cyclodextrins containing various drugs, such as levostatin, meloxicam, acyclovir, ciprofloxacin, ketoprofen, etc., were obtained [17–21]. Also, there are examples of “stimulus-sensitive” non-woven fibers with drugs (capable of changing the physicochemical properties of the material depending on pH, temperature, light, etc.) based on polylactide, polycaprolactone, polyethylene glycol, polyvinylpyrrolidone containing antibiotics—ciprofloxacin, doxorubicin, vancomycin, tetracycline, and anti-inflammatory drugs (ketoprofen, ibuprofen) [22–25].

Particularly in demand and promising are ESF products obtained from resorbable polymeric materials, among which are polymers of hydroxy derivatives of alkanic acids, the so-called polyhydroxyalkanoates (PHA). These polymers, along with polylactides and polyglycolides, have great potential for practical applications in various fields, from utilities and agriculture to reconstructive medicine and pharmacology. PHA are resorbable “green” bioplastics of microbiological origin, which have a unique set of properties, including high biocompatibility, lack of hydrolysis in aqueous media, long-term degradation in biological media *in vitro* and *in vivo*, thermoplasticity, piezoelectric effect, the possibility of processing into products from various phase states with available methods, as well as a wide range of physical and mechanical characteristics, which depend on the chemical composition of various types of PHA [26–35]. Through the efforts of a large number of scientific teams and companies that research and develop PHA in many countries, the possibility of obtaining materials and medical products from PHA for general, abdominal and cardiovascular surgery, orthopedics and traumatology, dermatology, etc., [36–42] has been shown. A line of Tephra Lexington, (Lexington, MA, USA) products (suture material, mesh endoprostheses, smooth membranes) received FDA approval for clinical use [43,44].

The development of the method of electrostatic molding in relation to PHA was started on the example of the most mastered and studied types of PHA—3-hydroxybutyric acid homopolymer (P3HB) and copolymers of 3HB monomers with 3-hydroxyvalerate monomers P(3HB-co-3HV) relatively recently, in 2005–2006 [45–47]. Further on, the range of studied types of PHA expanded. Nanofibers from other types of PHA, less crystalline compared to P(3HB), more elastic and attractive for use, were obtained and studied. These are copolymer nanofibrous membranes made of poly(3-hydroxybutyrate-co-3-hydroxyhexanoate) P(3HB-

co-3HHx), and poly(3-hydroxybutyrate-co-4-hydroxybutyrate) P(3HB-co-4HB) [48–50]. In a number of works, the characteristics of the ESF of nanomatrices from 3 and 4 types of PHA were obtained and studied in a comparative aspect: P(3HB), P(3HB-co-3HV), P(3HB-co-3HHx), and P(3HB-co-4HB). Morphology, diameter of the fibers, mechanical properties, and dependence on the chemical composition of PHA and the type of ultrathin fibers formed (oriented or non-oriented) were described [51,52].

Extensive studies have shown the high properties and suitability of PHAs electrospun fibrous scaffolds for growing cells of various origins: fibroblasts, osteoblasts, bone marrow mesenchymal stem cells, etc. [47,51,53–57]. It has been established that the composition and structure of nanomatrices, as well as the level of fiber orientation (aligned or random) affect the development and morphology of eukaryotic cells [58,59]. Thus, aligned fibers are more favorable for attachment and proliferation of osteoblasts, vascular endothelial cells, and neurons than randomly oriented fibers [48,55,60]. Fibroblastic cells develop more actively on more porous scaffolds formed by non-oriented fibers [58,61].

Relatively recently, studies of the effectiveness of the use of non-woven PHA nanomatrices for drug deposition have intensified [42]. Such studies were carried out with loading of ESM nanomatrices from P(3HB) with various antibiotics, including gentamicin sulfate, kanamycin sulfate, and levofloxacin [62–64]. The results obtained in vitro in cultures of pathogenic microorganisms by the disk diffusion method demonstrated the antibacterial activity of nanomatrices against *Micrococcus luteus*, *Serratia marcescens*, *Escherichia coli* [63], and *Staphylococcus aureus* [64].

A series of works describes PHA nanomatrices fabricated by the ESF method, loaded with nanosilver as an antibacterial agent. It has been shown that silver nanoparticles and graphene in the composition of nanofibers of P(HB-co-HHx) copolymers are effective in suppressing the development of *S. aureus* and *E. coli* [65]. Encapsulated hexagonal boron nitride in PHA/chitosan nanocomposites showed significant antibacterial activity against multi-resistant *E. coli* and methicillin-resistant *S. aureus* (MRSA) [66]. Nanofibers 5–13 nm in diameter obtained from the P(HB-co-HV) copolymer and loaded with silver nanoparticles (AgNP) exhibited antibacterial activity in vitro in cultures of *Staphylococcus aureus* and *Klebsiella pneumoniae* [67].

In a recent study, it was shown that the inclusion of the nitric oxide (NO) donor S-nitrosoglutathione in the composition of nanofibers from the P(3HB) copolymer with polylactide (P3HB/PLA) is effective, since the use of such fibers has a dual effect and exhibits antibacterial and antithrombotic activities [68]; at the same time, it was found that NO released from nanofibers prevents cell adhesion and effectively reduces the number of *S. aureus* and platelets, respectively, by 80% and 65%. A similar positive effect of PHA-based nanofibers in combination with drugs has been shown for the healing of skin wounds [69]. The authors of this work fabricated a nanofibrous matrix of poly-3-hydroxybutyric acid and sodium alginate according to the core-shell principle as a protective scaffold for skin tissue regeneration in an excised wound model. Arginine and layered bacitracin double hydroxides were incorporated into the core and shell of the nanofiber matrix using coaxial electrospinning. The designed system promoted synergistic controlled delivery of L-arginine and bacitracin, playing an important role in protein synthesis, cell signaling, and infection control at the wound site. The biocompatibility of the composite matrix was confirmed in vitro on a culture of dermal fibroblasts; in vivo studies revealed a synergistic effect of both components and active healing of model wounds. Li et al. [70] developed a PHA-based nanofiber with a core-shell structure containing a biocide. The authors of the work showed that the biocide (dodecyltrimethylammonium chloride) is released only under the influence of an irritant (the presence of pathogenic bacteria); the nanofiber is triggered by irritants and the effective release of the biocide takes place only when a pathogen appears in the wound, which leads to a weakening of the growth of these bacteria. Using *Pseudomonas aeruginosa* and dodecyltrimethylammonium chloride, it has been shown that PHA-based nanofibers effectively release this biocide in the presence of a pathogen

and purposefully inactivate it. The mechanical properties of the membrane are close to those of human skin.

These results, while very few, allow us to conclude that the simultaneous presence of a complex of drugs in such nanosystems is certainly more effective, since it can impart a more pronounced drug effect to such a nanomatrix and promote more active tissue genesis, on the one hand, and, on the other hand, also suppress infection in case of infected wounds. However, there is a concern that the presence of several drugs in such nanosystems, including those with antibacterial and cytostatic activity, may have a negative effect on the proliferation of cells at the site of the defect and inhibit reconstructive formation of tissue. Therefore, when designing such systems, studies are needed to reveal the effects of deposited drugs not only on the suppression of pathogens, but also on the growth of cells involved in the regeneration, as well as pathogens.

This determined the purpose of this work, which presents the results of the design of non-woven membranes from resorbable low-crystalline and highly elastic copolymers of 3- and 4-hydroxybutyrate, P(3HB-co-4HB), loaded with drugs of various nature by the ESF method, the study of their characteristics and biological activity in relation to pathogens (*E. coli* and *St. aureus*) and fibroblast cells.

2. Materials and Methods

2.1. Materials

We used a copolymer of 3-hydroxybutyric-co-4-hydroxybutyric acid [P(3HB-co-4HB)] synthesized by the natural strain *Cupriavidus necator* B-10646 according to our own developed technology at the Institute of Biophysics of the Siberian Branch of the Russian Academy of Sciences [71] with a ratio of 3HB and 4HB monomers 74 and 26 mol.%, respectively, weight average molecular weight 640 kDa, number average molecular weight, 256 kDa, polydispersity 2.5, degree of crystallinity 49%, melting temperature 159 °C, thermal degradation temperature 250 °C. The structural formula of [P(3HB-co-4HB)] is shown in Figure 1.

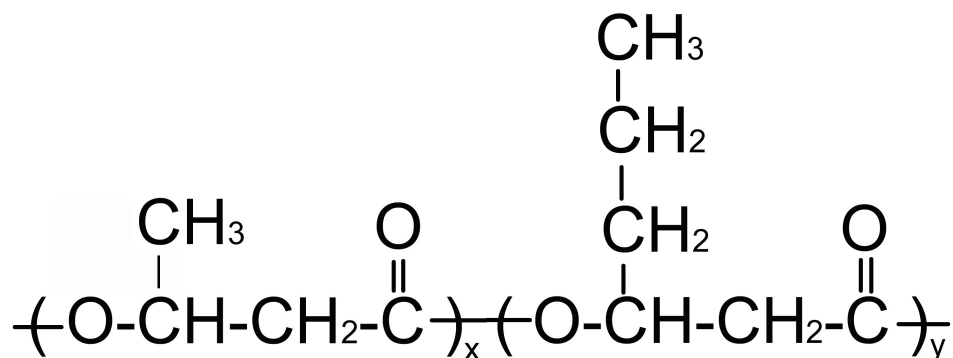
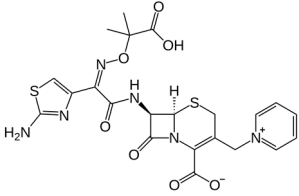
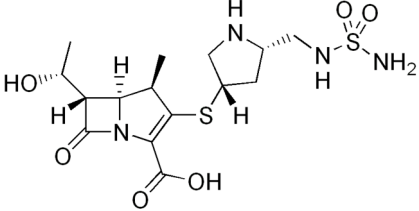


Figure 1. Structural formula of [P(3HB-co-4HB)].

Copolymer synthesis method and methods for studying of physicochemical properties (molecular weight (M_w, M_n, Đ) and temperature (T_{melt}, T_{degr}) characteristics, degree of crystallinity (C_x) have been described in detail earlier [72].

Drugs with different mechanisms of action were used as medicines (Table 1): antibiotics—Sanocel[®] (doripinem) (JSC Pharmsintez, Bratsk, Russia) and Protozidim[®] (cef-tazidime) (JSC Pharmsintez, Bratsk, Russia), as well as Actovegin[®] (Takeda Austria GmbH, Vienna, Austria)—the drug activates the metabolism in tissues, improves trophism and stimulates regeneration processes; it is widely used in Russia in clinical practice for intravenous injections and as part of gels and ointments for wound healing (Table 1).

Table 1. Drugs taken for inclusion in the ESF non-woven membranes and their mechanism of action.

Drug	Structural Formula	Mechanism of Action
Ceftazidime		Ceftazidime is a third-generation cephalosporin antibiotic. It has a bactericidal effect, disrupting the synthesis of the bacterial cell wall. It has a high natural activity against gram-negative bacteria and is not inactivated by many β -lactamases. Degraded by extended spectrum β -lactamases and class C β -lactamases.
Doripinem		Antibiotic of the beta-lactam group. It has a wide spectrum of antimicrobial activity, including many Gram-positive and Gram-negative aerobes and anaerobes. Resistant to penicillinases and cephalosporinases. The mechanism of action is based on the binding of specific beta-lactamotropic proteins of the cell wall and inhibition of peptidoglycan synthesis, leading to the lysis of sensitive bacteria.
Actovegin	* It is a deproteinized hemoderivative of calf blood, which includes amino acids, oligopeptides, nucleosides, intermediate products of carbohydrate and fat metabolism, antioxidant enzymes, electrolytes, microelements.	Antihypoxant has three types of effects: metabolic, neuroprotective and microcirculatory; activates the metabolism in tissues, improves trophism, and stimulates the regeneration processes; is widely used in Russia in clinical practice in the form of intravenous injections and as part of gels and ointments for wound healing.

*—due to the complexity of the composition, the structural formula is not given.

2.2. Obtaining Non-Woven Membranes by Electrostatic Molding of a Polymer Solution

To obtain a 7% solution of P(3HB-co-4HB) copolymer, the solvent hexafluoro-2-propanol (HFIP, 1,1,1,3,3,3-hexafluoro-2-isopropanol) (Sigma-Aldrich, St. Louis, MO, USA) was used. Non-woven membranes formed by ultrafine fibers have been obtained using a Nanon 01A automatic setup (MECC Inc., Fukudo, Japan). For getting randomly oriented-fibers, ESF were collected on a flat steel plate; a collector was covered with aluminum foil to collect ultrafine fibers more effectively. The polymer solution was poured into a plastic syringe (12.5 mm inside diameter); the process has been described in detail earlier [52]. The process parameters have the following settings: electrode distance 250 mm, syringe diameter 12.5 mm, needle diameter 1 mm, voltage deference 30 kV, feed rate 2 mL/h.

To obtain non-woven membranes containing drugs, solutions of P(3HB-co-4HB) with doripinem, ceftazidime, or actovegin were preliminarily prepared. These solutions were prepared by dissolving the polymer and drug in 10 mL of HFIP, followed by stirring with a magnetic stirrer for 4 h. The drug content was 10% by weight of the polymer in all variants. Next, a freshly prepared polymer solution with a drug in a volume of 4.0 mL was transferred into a syringe installed in a horizontal position in a dosing device. The conditions for obtaining non-woven membranes with drugs were similar to the conditions for obtaining non-woven membranes from a solution of P(3HB-co-4HB).

The products obtained by ESF were dried until the solvent was completely evaporated in a vacuum desiccator (Labconco, Kansas City, MO, USA) and stored at 4 °C. Figure 2 shows the scheme of operations for obtaining ESF non-woven membranes.

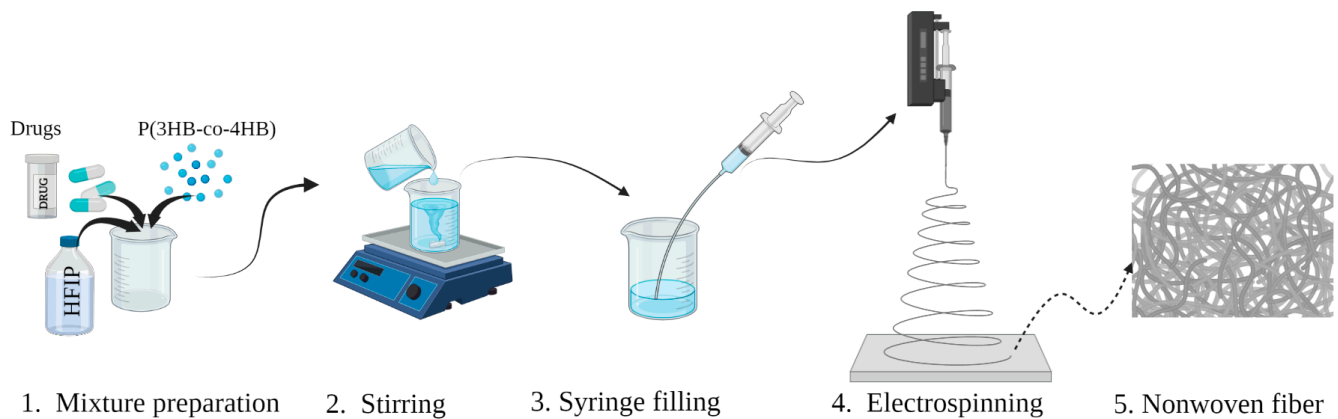


Figure 2. Schematic representation of the process of obtaining non-woven membranes containing drugs by the ESF method.

2.3. Characteristics of Non-Woven Membranes P(3HB-co-4HB) Loaded with Drugs

The thickness of the formed ESF membranes was determined with a LEGIONER EDM-25-0.001 electronic micrometer (Legioner, Xi'an, China) (at least in 5 points for each sample). The surface characteristics were evaluated using a DSA-25E contact angle measuring machine (Krüss, Hamburg, Germany) using the DSA-4 software for Windows. To find the contact angles of wetting, the frame of the video recording of the drop after its stabilization was processed in the semi-automatic mode by the "Circle" method built into the software package. From the obtained values, the free surface energy, its dispersive and polar components (mN/m) were calculated by the Ouns-Wendt-Rabel-Kjellble method [73,74].

The study of the microstructure of the surface of non-woven membranes was performed using a scanning electronic microscope TM4000 Plus (Hitachi, Tokyo, Japan) in the BSE mode with an acceleration voltage of 20 kV and maximum current equipped with an EDX XFlash Detector 630 Hc (Bruker, Mannheim, Germany). Prior to microscopy, the samples were sputtered with platinum (at 25 mA, for 60 s) using an EM ACE200 (Leica, Vienna, Austria). Using SEM images of ESF matrices, the size distribution and average diameter of ultrathin fibers were determined using the Image J v1.53k digital image analysis software package. Packing density was calculated indirectly by measuring the weight of membrane samples per unit area.

IR spectroscopy with NICOLET 6700 FT-IR spectrometer (Thermo Scientific, Waltham, MA, USA) was used to study the nature of the interaction between the copolymer [P(3HB-co-4HB)] and drugs. IR spectra were taken in the range 400–4000 cm^{-1} with the Smart Orbit accessory by the attenuated total reflection (ATR) technique. The absolute value of the maximum permissible error is $\pm 0.01 \text{ cm}^{-1}$.

2.4. Dynamics of Drug Release from Non-woven P(3HB-co-4HB) Membranes In Vitro

Non-woven P(3HB-co-4HB) membranes containing antibiotics were used to study the efflux dynamics of doripinam and ceftazidime. Samples of known weight were placed in sterile tubes with phosphate-buffered saline (PBS, pH 7.4). The flasks were exposed in a thermostat at 37 °C. Antibiotics releases from non-wovens were determined with UV-VIS spectrophotometry (Genesys 10S UV-VIS Spectrophotometer, Thermo scientific, Waltham, MA, USA) at 297 nm for doripinam and 256 nm for ceftazidime within 16 days. The concentrations of the released antibacterial drugs were calculated from the intensity of absorbance. The release experiment was repeated three times for each sample and average values were considered. In order to explore the mechanism of antibacterial drug release in electrospun samples, Zero-order, First-order, Higuchi, Hixon-Crowell and Korsmeyer-Peppas models were examined [75,76].

To quantify the content of doripinam and ceftazidime in non-woven membranes, samples weighing 10.0 mg were dissolved in 10.0 mL of HFIP until the antibiotic and the

polymer base were completely dissolved. The resulting solution was stirred for an hour, followed by analysis on a UV spectrophotometer (Genesys 10S UV-VIS Spectrophotometer, Thermo scientific, Waltham, MA, USA). The readings were compared to a calibration curve generated using standard samples of doripinem and ceftazidime in HFIP. Absorption was recorded and the actual content of antibiotics in non-woven membranes was determined.

2.5. Antibacterial Properties of Non-Woven Membranes P(3HB-co-4HB)/Antibiotics

The antibacterial activity of non-woven membranes containing doripinem or ceftazidime was assessed by the disk diffusion method [77]. Membrane cutouts 6 mm in diameter were placed on a Mueller-Hinton agar plate inoculated with *Escherichia coli* or *Staphylococcus aureus* at a density of 0.5 McFarland. The plates were incubated at 37 °C for 24 h and then the zone of inhibition of bacterial growth was determined by measuring the diameter of the transparent circle on the agar formed around the membrane cutouts.

2.6. Evaluation of Non-Woven Membranes as Scaffolds for Cell Growth In Vitro

The ability of non-woven membranes loaded with drugs to possess cell adhesion and proliferation was studied in a culture of linear mouse fibroblasts NIH 3T3. Presterilized cuts 6 mm in diameter were placed in 96-well culture plates (Corning Costar, New York, NY, USA) and seeded with fibroblasts at a density of 5×10^4 cells/cm². Cultivation was carried out according to the standard method in DMEM medium with the addition of 10% fetal calf serum and 1% antimycotic antibiotic solution (Gibco, Invitrogen) in a humid atmosphere (5% CO₂) at a temperature of 37 °C in a CO₂ incubator (New Brunswick Scientific, Edison, NJ, USA) within 72 h.

Cell morphology and nucleus circularity were studied using scanning electron microscopy and staining of the cytoplasm and nuclear DNA with fluorescent dyes FITC and DAPI, respectively (Sigma-Aldrich). To obtain SEM images, the cells were fixed with 4% glutaraldehyde for 1 h, then counterstained with 1% OsO₄ solution, and then dehydrated with a battery of alcohols from 10 to 100%. Before microscopy, the samples were sputtered with platinum and analyzed using a Hitachi TM4000 scanning electron microscope (Japan).

The number of viable cells was assessed in the MTT assay based on the reduction of 3-(4,5-dimethylthiazol-2-yl)-2,5-diphenyltetrazolium bromide (Sigma) by cell dehydrogenases to purple MTT-formazan crystals. In the wells with cultured cells, the medium was changed to a freshly prepared medium containing 5% MTT solution. After 4 h of incubation, the disks were transferred to clean plates, DMSO was added to dissolve the formed formazan crystals. After 30 min, the stained solutions were transferred to a 96-well plate and the optical density was measured at a wavelength of 550 nm using a Bio-Rad 680 microplate reader (Bio-Rad Laboratories Inc., Hercules, CA, USA).

2.7. Statistics

Statistical analysis was carried out by Microsoft Excel and shown as mean standard deviation using Student's *t*-test. Difference with *p* values <0.05 was considered statistically significant.

3. Results

3.1. Characterization of ESF Non-woven Membranes P(3HB-co-4HB)/Drug

To obtain non-woven membranes by electrostatic spinning of a solution, a copolymer containing monomers of 3- and 4-hydroxybutyrate [P(3HB-co-4HB)] was taken. The choice of the polymeric material is due to the excellent properties inherent in this type of PHA [78,79]. The reduced crystallinity of this copolymer makes it possible to obtain the most durable products, characterized by the highest rates of elasticity (elongation at break up to 1000%), registered in products from all other types of PHA. The absolute biocompatibility of this type of PHA in vitro and in vivo [78] is due to the fact that butyric acid monomers are "invisible" to the immune system, since they are contained in the human

body (in the brain, heart, lungs, liver, kidneys, muscles) [80]. The half-life of the copolymer is about 35 min and is broken down in the body through the Krebs cycle and then converted into carbon dioxide and water [81]. That is, they are less acidic than α -hydroxy acids: glycolic acid (pH 3.83 at 25 °C [82,83] and lactic acid pH 3.86 at 20 °C [84], which are released from PGA and PLLA implants during their bioresorption in vivo, respectively. This copolymer degrades more slowly than PGA, but faster than PLLA, and PCL [78], as well as known types of PHA [85]. Therefore, a very fast bioresorption in vivo precludes the formation of rough fibrous capsules around their implants.

Solutions of the P(3HB-co-4HB) copolymer in HFIP were preliminarily prepared. Next, a weighed portion of the drug at the rate of 10% by weight of the polymer was added to the polymer solution, and the finished solution was thoroughly mixed. The electrospinning process was carried out at the parameters worked out earlier for PHA [52]. To get randomly oriented ESF, membranes fibers were collected on a flat steel plate.

Figure 3 shows SEM images of the drug-loaded non-woven membranes; Table 2 shows their characteristics. The analysis of SEM images allows us to conclude that the non-woven membranes in the control obtained from the copolymer, as well as the experimental samples loaded with drugs are formed by microfibrils heterogeneous in size. Visually, the surface of all types of ESF membranes was relatively smooth without markable defects. Using the Image J software for analysis and image processing, it was found that the diameter of ESF matrices in the control (containing no drugs) varied from 1.4 μm to 3.7 μm , with an average diameter of $2.7 \pm 0.5 \mu\text{m}$.

Table 2. Characteristics of ESF membranes P(3HB-co-4HB)/drug.

Matrix Thickness, mm	Fiber Diameter, μm	Average Fibers Diameter, μm	Fiber Bulk Density, g/cm^3
		P(3HB-co-4HB)	
0.185	1.4–3.7	2.7 ± 0.5	0.4
		P(3HB-co-4HB)/doripinim	
0.120	4.3–9.2	6.8 ± 0.9	0.9
		P(3HB-co-4HB)/ceftazidime	
0.155	0.1–2.7	1.2 ± 0.6	0.4
		P(3HB-co-4HB)/actovegin	
0.160	0.2–2.6	1.1 ± 0.5	0.6 ± 0.1

The addition of drugs to the P(3HB-co-4HB) solution during electrospinning had different effects on the properties of the resulting ESF membranes. Thus, the samples loaded with Ceftazidime had fibers that were smooth in structure, without deformations, drops, and visible crystals of the drug on the surface. The size distribution of fibers over diameters for this sample varied from 0.1 to 2.7 μm ; 60% of the fibers in the sample had a diameter of 0.9–1.4 μm . The average fiber diameter was $1.2 \pm 0.6 \mu\text{m}$, which is two times less compared to the control samples. The fibers in the samples of non-woven membranes loaded with Actovegin had similar values; their mean diameter was $1.1 \pm 0.5 \mu\text{m}$ (Table 2 and Figure 3).

However, samples of ESF membranes loaded with doripinim at the same concentration had different characteristics. Visually, the membranes had a denser structure and were formed by larger fibers, the size of which varied in a wide range, from 4.3 to 9.2 μm , including as a result of adhesion of thinner fibers. The average fiber diameter was $6.8 \pm 0.9 \mu\text{m}$. Small clusters of drug crystals were observed on the membrane surface. These differences seem to be related to the properties of the drug. There is evidence in the literature that uneven dispersion of a drug in a polymer solution leads to the formation of drug crystals or particles on the surface of membranes, which can induce adhesion of the membrane fibers. In addition, drugs can change the viscosity of the polymer solution and lead to a decrease in the electrical conductivity of the solution, which in turn can increase the diameter of the fibers and change their structure [86,87].

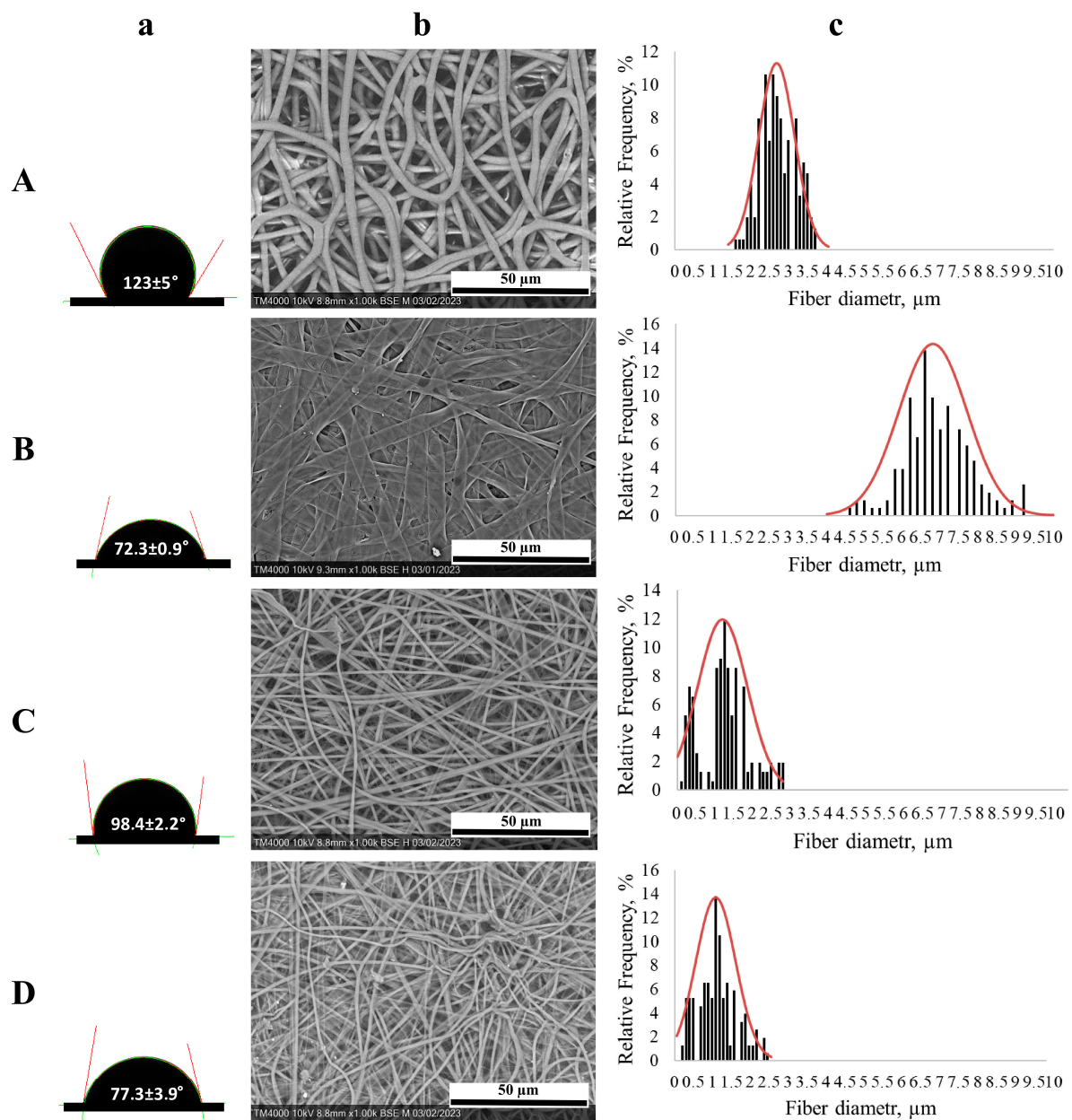


Figure 3. Characteristics of non-woven membranes containing drugs: A—P(3HB-co-4HB), B—P(3HB-co-4HB)/doripinim, C—P(3HB-co-4HB)/ceftazidime, D—P(3HB-co-4HB)/actovegin. Contact angles of wetting with water (a), SEM images (b), size distribution of fibers in membranes (c). Bar is 50 μm .

It is known that the properties of non-woven membranes largely depend on the density of the polymer solution, the type of drug, and, in general, on the parameters of the ESF process [56,88–90]. For example, in [62], ESF membranes were obtained from a mixture of polyvinylidene fluoride and poly-3-hydroxybutyrate and chitosan containing Gentamicin at concentrations of 1, 2, and 3%. The average diameter of ultrathin fibers varied from 100 to 207 μm depending on the composition and ratio of components in the initial solution. In another work [63], non-woven fiber mats were also obtained from P(3HB) containing Levofloxacin (1.0% of the polymer weight). The resulting ESF membranes had different morphology, including the presence of pores, filamentous/spherical formations on the fibers, depending on the density of the polymer solution. When using P(3HB) solutions in HFIP of various concentrations, the fiber diameter varied from 190 to 700 nm. The introduction of the antibiotic kanamycin into the polymer solution led to the formation of

non-woven membranes, on the surface of which areas of accumulation of the drug were observed [64]. In [91], the dependence of the fiber diameter on the content of tetracycline was shown, which was used to obtain membranes by electrospinning from a P(3HB-co-3HV) copolymer with the addition of nanocellulose crystals. The average diameter of the fibers obtained from a 5% polymer solution was 230 nm. An increase in the antibiotic concentration to 15% was accompanied by a decrease in the average fiber diameter to 170 nm due to an increase in the conductivity of the polymer solution and stretching of the jet during electrospinning. These results indicate that the morphology and diameter of ultrathin fibers in the ESF process is a variable value that can be controlled by changing not only the parameters of the spinning process, but also by varying the composition of the polymer solution, and the type and concentration of the drug.

An important feature for non-woven membranes is the hydrophilic-hydrophobic balance of the surface, the indicator of which is the value of the contact angle of wetting the surface with liquids. The results of determining the contact angle of wetting the surface of non-woven membranes with distilled water and the values of the free surface energy and its components (dispersion and polar components) calculated on its basis are given in Table 3.

Table 3. Surface properties of P(3HB-co-4HB)/drug non-woven mats.

Contact Angle of Wetting with Water [°]	Free Surface Energy, mN/m	Dispersion Component, mN/m	Polar Component, mN/m
	P(3HB-co-4HB)		
123 ± 5	47.4 ± 0.4	44.1 ± 0.2	3.3 ± 0.2
	P(3HB-co-4HB)/doripinim		
72.3 ± 0.9	38.1 ± 0.4	27.4 ± 0.3	10.7 ± 0.1
	P(3HB-co-4HB)/ceftazidime		
98.4 ± 2.2	31.8 ± 0.3	31.1 ± 0.3	0.7 ± 0.1
	P(3HB-co-4HB)/actovegin		
77.3 ± 3.9	36.7 ± 1.1	29.2 ± 0.7	7.6 ± 0.3

The highest value of the contact angle of the surface of non-woven membranes ($123 \pm 5^\circ$) was registered for the control samples (not containing drugs). Non-woven membranes containing drugs had a lower angle. The decrease in the index was 25° for the sample with ceftazidime ($98.4 \pm 2.2^\circ$). The value of the contact angle for membranes with actovegin decreased more significantly, to $77.3 \pm 3.9^\circ$. The membranes with doripinim had the minimum angle value ($72.3 \pm 0.9^\circ$), which is 40% lower than the control.

The results of calculations of the surface free energy (SFE) and its components indicate that the highest SFE value was obtained in the case of control samples of membranes (47.4 ± 0.4 mN/m). The lowest value of the indicator was noted for membranes with Ceftazidime (31.8 ± 0.3 mN/m). Similarly, significant differences in the values of the polar component were obtained—the highest value was observed in membranes with doripinim (10.7 ± 0.1 mN/m); and the smallest in the sample with ceftazidime (0.7 ± 0.1 mN/m). According to the dispersion component, it was noted that it determines most of the SFE, while accounting for 72 and 80% for samples with doripinim and actovegin, respectively, and 98% for membranes with ceftazidime (the value for control samples was determined at the level of 93%).

By the literature data, the addition of hydrophilic polymers or drugs to PHA solutions in the process of obtaining non-woven membranes leads to a decrease in the contact angle of wetting with water [92,93]. The addition of silk fibroin to P(3HB-co-4HHx) resulted in a decrease in the water contact angle to 54° compared to the non-woven membrane from P(3HB-co-4HHx), for which the water contact angle was 119.6° . In [91], a decrease in this index was observed for non-woven membranes obtained with the addition of nanocrystalline cellulose and Tetracycline. The contact angle of wetting with water for non-woven membranes obtained from the P(3HB-co-3HV) copolymer (without preparations)

was 55° , while the membranes containing nanocrystalline cellulose and antibiotic had a smaller angle (46°).

In general, the results of this work are consistent with the publications and indicate that the addition of drugs to non-woven membranes obtained from P(3HB-co-4HB) by the ESF method positively affects the properties of the membrane surface, namely, increases their hydrophilicity.

To identify the nature of the interaction of components in non-woven membranes and determine what the “copolymer/drug” system is, a physical mixture or a chemical interaction product, IR spectroscopy was used to determine this (Figure 4).

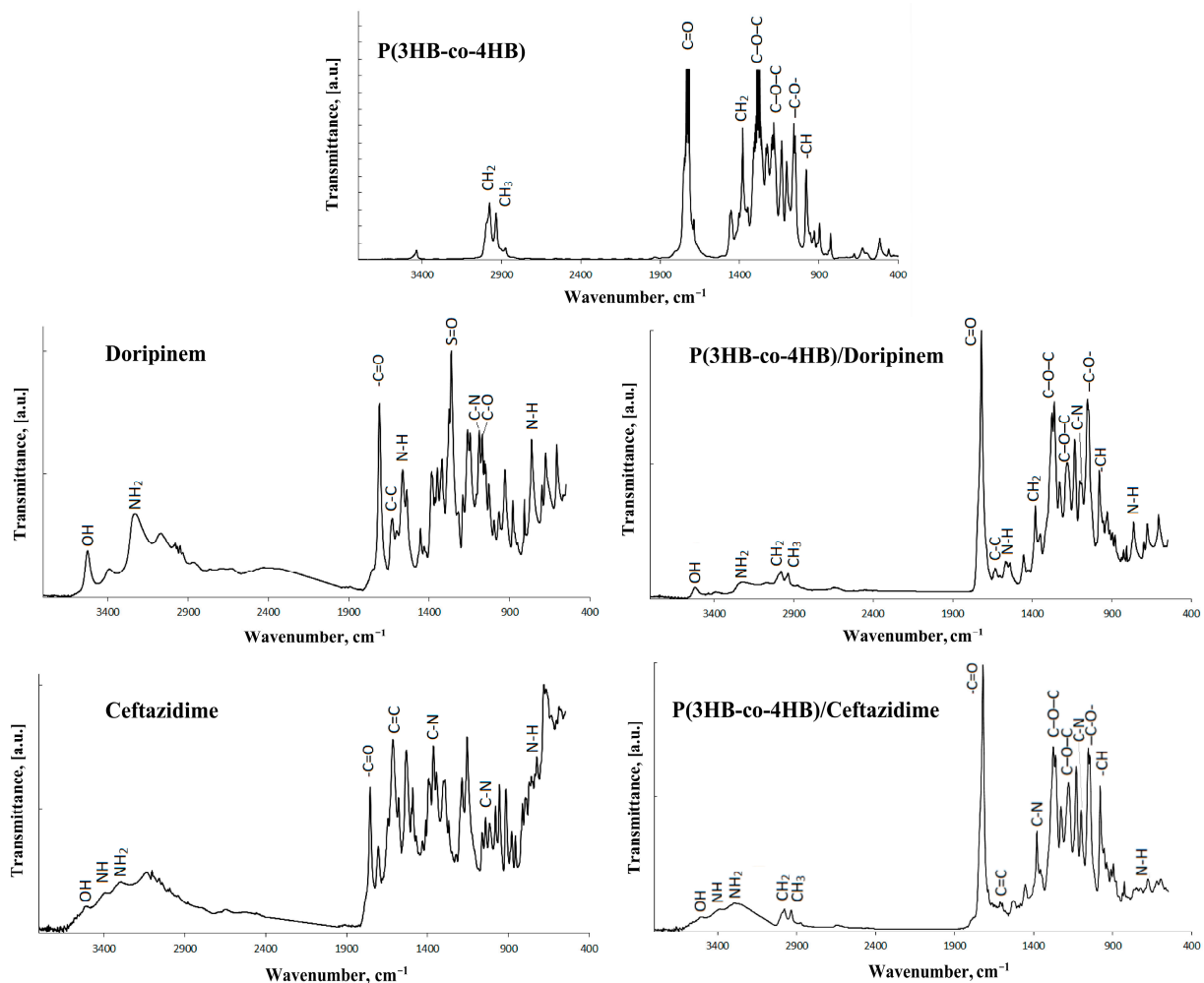


Figure 4. IR spectra: P(3HB-co-4HB), drugs and composite ESF membrane P(3HB-co-4HB)/drug.

The absorption bands (1731 and 1720 cm^{-1}) are assigned to the stretching vibrations of the amorphous and crystalline carbonyl groups, respectively. The intense band at 1278 cm^{-1} in the IR spectrum of P(3HB-co-4HB) corresponds to C–O–C stretching vibrations. There is asymmetric stretching vibration of the C–O–C group, which is a well-known amorphous band at 1183 cm^{-1} . There are absorption bands of asymmetric stretching vibrations of CH_3 - and CH_2 -groups (2974 , 2931 cm^{-1}); the absorption band at 1378 cm^{-1} is assigned to bending vibrations of CH_2 groups; the band of medium intensity at 1059 cm^{-1} is attributed to the stretching vibrations of the –C–O– bond. The band at 978 cm^{-1} is attributed to deformation out-of-plane vibrations of –CH groups.

Ceftazidime(6R,7R,Z)-7-(2-(2-aminothiazol-4-yl)-2-(2-carboxypropan-2-yloxyimino)acetamido)-8-oxo-3-(pyridinium-1-ylmethyl)-5-thia-1-aza-bicyclo[4.2.0]oct-2-ene-2-carboxylate: The IR spectrum of Ceftazidime characteristic absorption bands of C=O groups were

recorded as stretching vibrations of the carbonyl group (1750 cm^{-1}), and a set of absorption bands in the range $1529\text{--}1616\text{ cm}^{-1}$ were assigned to bending vibrations of the C=C bond in the aromatic ring. In the frequency range $3660\text{--}3250\text{ cm}^{-1}$, there are absorption bands of bending vibrations associated with NH groups, which overlap with stretching vibrations of NH_2 (3250 cm^{-1}); and stretching vibrations of the associated alcohol OH groups (3510 cm^{-1}). The absorption band at 1360 cm^{-1} is assigned to axial bending vibrations of the C-N bond. In out-of-plane fan vibrations of the N-H group in lactams, there is a wide band of medium intensity in the range of $700\text{--}800\text{ cm}^{-1}$. The result obtained coincides with the data of other authors [94].

Doripinem is an antibiotic of the beta-lactam series; its key structure is 7-oxo-1-azabicyclo[3.2.0]hept-2-en-2-carboxylic acid. The specificity of the IR spectrum of doripinem is the presence of the following groups: R-C=O—stretching vibrations of the carbonyl group with a high intensity band (1710 cm^{-1}); stretching vibrations of the OH group (3521 cm^{-1}); out-of-plane fan vibrations of the N-H group in lactams is represented by a wide band of medium intensity (764 cm^{-1}); stretching vibrations of the N-H group in the sulfonamide (1562 cm^{-1}); bending vibrations of the NH group—a band of medium intensity (1627 cm^{-1}) and stretching vibrations of the free NH_2 group of medium intensity (3220 cm^{-1}). The intense band at 1261 cm^{-1} with a slight splitting corresponds to the stretching vibrations of the S=O group. High-intensity C-N stretching vibrations were recorded at 1085 cm^{-1} , which partially overlaps with the 1070 cm^{-1} C-O stretching band in alcohols. The medium-intensity band at 1625 cm^{-1} corresponds to C-C stretching vibrations in the rings. The taken spectrum of this antibiotic corresponds to the data of the work [95].

An analysis of the IR spectra of the obtained non-woven membranes P(3HB-co-4HB)/antibiotic (Figure 4) showed that no new significant absorption bands were found in the spectra of the samples, and there are bands characteristic of the original copolymer, and also antibiotics. This indicates the absence of chemical interaction between the components and the formation of new chemical bonds between them. Thus, constructed non-woven membranes prepared from solutions of a copolymer and antibiotics by the ESF method are physical mixtures.

3.2. Dynamics of Drug Release from ESF Membranes P(3HB-co-4HB)/Drug In Vitro

The release of drugs from non-woven membranes depends on the physicochemical properties of the material from which the fibers are obtained. In addition, the diameter and morphology of the fiber surface, the content of the drug in the matrix, as well as the chemical nature of the drug can affect the rate of outflow of drugs [41,96,97].

With regard to PHA, it is known that these polymers, in the absence of biological factors (enzymes, cells), practically do not undergo hydrolysis in liquid media [98–100]. As a rule, in physiological buffer solutions, for example, PBS (pH 7.4), PHA are destroyed very slowly, with a half-life of 56 weeks at $37\text{ }^\circ\text{C}$ [101]. Therefore, the efflux rate of drugs in an in vitro model medium that does not contain enzymes or cells will depend on the diffusion of the drug, and not on the degradation of the polymer matrix.

Actovegin consists of more than two hundred biological substances [102]; therefore, it is not possible to determine which of the drug components are active substances and to study their pharmacodynamics. In this regard, the dynamics of the release of drugs from the obtained non-woven membranes were studied only in relation to antibiotics (doripinem and ceftazidime). The results of the release of antibiotics from non-woven membranes, which were exposed to PBS solution (pH 7.4, $37\text{ }^\circ\text{C}$) for 16 days, are shown in Figure 5. The kinetic curves of the release of doripinem and ceftazidime had a two-phase character. At the first stage (6–48 h), the concentration of antibiotics in the medium increased, and starting from the 8th day (192 h), the outflow rate decreased.

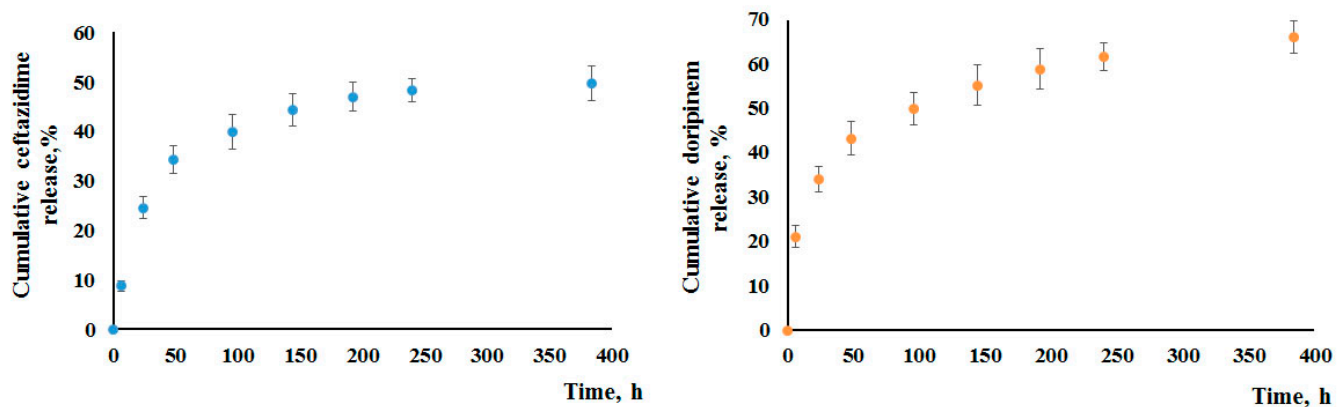


Figure 5. Drug release kinetics from P(3HB-co-4HB) non-woven membranes with 10% ceftazidime or doripinim (relative to the polymer weight) for 16 days of incubation in PBS.

During the first day (24 h), the amount of ceftazidime released from non-woven membranes was 24.5% of the deposited one. During the observation period from the second to the sixth day (48–144 h), the total yield of the drug reached 44%, while the release rate of ceftazidime over this period of time averaged 15.4 $\mu\text{g}/\text{day}$. After 192 h, the curve flattened, showing that the rate of antibiotic release decreased and averaged 2.1 $\mu\text{g}/\text{day}$. The kinetic curve describing the dynamics of release of the second antibiotic, doripinim, from non-woven membranes shows a higher concentration of the antibiotic in the model medium on the first day of observation, which was 34% of the initial content in the membrane. In the next observation period (48–144 h), the total yield of doripinim reached 55%, the average rate of release of this antibiotic at this stage was 32.5 $\mu\text{g}/\text{day}$. This exceeded the release rate of ceftazidime by almost two times over the same period of time. Starting from the 8th day (192 h) until the end of the experiment, the release rate of doripinim was on average 9.3 $\mu\text{g}/\text{day}$. By the end of the experiment, the total yield of doripinim was 65% of that included in the mass of membrane. This value is higher than that for ceftazidime (49.6%).

A higher concentration of doripinim in the model medium on the first day of observation may be due to the fact that part of the antibiotic was located on the surface of non-woven membranes in the form of individual drug particles (Figure 3), which easily diffused into the buffer. In addition, a slight increase in doripinim efflux rate may be due to differences in the physicochemical properties of antibacterial drugs. The molecular weights of doripinim and ceftazidime are similar and are 420.5 g/mol and 547 g/mol, respectively. However, the water solubility index of doripinim is higher (3.13 mg/mL) compared to ceftazidime (0.006 mg/mL) [103]. Higher solubility could increase the release of doripinim from non-woven membranes.

According to the literature data [86,91], the outflow of drugs from non-woven membranes obtained from PHA copolymers into a model medium at the first stage can be associated with the diffusion of drug molecules from the outer layers of polymer membranes and from more amorphous regions of the polymer. Further, there is a decrease in the rate of outflow of drugs, which the authors explain by the fact that the diffusion of aqueous solutions into the internal regions of the polymer mats is hindered due to the crystalline regions of the polymer.

Five mathematical models were used to describe the mechanism of antibiotic release from non-woven membranes: zero order, first order, Higuchi, Hixson–Crowell, and Korsmeyer–Peppas. Based on the above models, the values of the release constant and the coefficient of determination (R^2) were calculated.

Based on the obtained data (Table 4), the kinetics of doripinim efflux from the membranes can be adequately described using two models (Higuchi and Korsmeyer–Peppas), as indicated by high approximation coefficients exceeding 0.9 (0.93 and 0.997), respectively.

In the case of a non-woven membrane containing ceftazidime, the highest approximation coefficient (0.997) was obtained when calculating according to the Korsmeyer-Peppas model. In addition, according to the Korsmeyer-Peppas model, the value of “n” indicates the mechanism of drug release. Values of n from 0.5 to 1.0 indicate a superposition of two processes (anomalous transfer), which is characterized by a combination of the diffusion mechanism and the erosion mechanism, while the release degree index of 0.5 or less has a diffusion character and obeys Fick’s laws [104]. In general, it is shown that the release of doripinem and ceftazidime proceeds smoothly, while there is no pronounced so-called “peak effect”. The results correspond to the data of other authors. Thus, in [62], when studying the release of gentamicin from a bilayer non-woven membrane P(3HB-co-3HV)/chitosan, it was shown that in the first hours, the outflow of gentamicin reached 30%, followed by a decrease in the antibiotic release rate. Depending on the composition of the composition, the total yield of gentamicin varied from 60 to 80%. Using the Korsmeyer-Peppas model, the authors explained the mechanism of gentamicin outflow by Fick’s law. A similar mathematical dependence was observed by the authors in [91], who studied the kinetics of tetracycline outflow from a composite nanomembrane based on P(3HB-co-3HV) with the addition of cellulose nanocrystals. Using various mathematical models, the authors established the adequacy for describing the obtained dependences of the Korsmeyer-Peppas model. In this case, the mechanism of tetracycline release can be associated with Fick diffusion or with abnormal transfer processes, depending on the ratio of components in the composite membrane.

Table 4. Release parameters of drugs from P(3HB-co-4HB)non-woven membranes in PBS buffered solution.

Drug	Zero-Order		First-Order		Higuchi		Hixon-Crowell		Korsmeyer-Peppas	
	R ²	K ₀ × h ⁻¹	R ²	K ₁ × h ⁻¹	R ²	K _H × h ^{-0.5}	R ²	K _S C ^(h-1/3)	R ²	n
DOR	0.66	0.14	0.70	−0.0009	0.93	2.56	0.82	−0.007	0.99	0.25
CEF	0.63	0.11	0.85	−0.0005	0.84	2.26	0.67	−0.005	0.98	0.24

DOR—doripinem, CEF—ceftazidime.

The gradual release of drugs from non-woven membranes obtained from P(3HB) in composition with pluronic and PLGA loaded with doxycycline and dipyrindamoom is described in [92]. In [63], the dynamics of the release of levofloxacin from non-woven membranes obtained from P(3HB) was studied, and it was shown that on the first day, the antibiotic yield was 14–20% of that included, followed by a slowdown in the outflow rate. The total yield of gentamicin by day 13 was 30–32.5%. The literature also describes examples of faster antibiotic release from non-woven membranes. Thus, in [62], the yield of kanamycin in phosphate-buffered saline from non-woven membranes made of P(3HB) after 2 h was more than 70%, and after 8 h it reached 100%. The authors explained the rapid outflow of the drug by the fact that clarithromycin was unevenly dispersed in the solution with the polymer, as a result of which the drug was mainly localized on the surface of the fibers forming the membranes and easily diffused into the model medium.

In the present work, it is shown that the outflow of antibiotics from non-woven membranes made from the P(3HB-co-4HB copolymer) occurs smoothly without sharp outbursts and its dynamics are influenced by the type of deposited antibiotic.

3.3. Antibacterial Activity of Non-Woven Membranes P(3HB-co-4HB)/Drug

Drug-loaded non-woven membranes are considered promising agents for the treatment of skin and soft tissue injuries, including those complicated by infection. To date, the antimicrobial action and mechanism of action of drugs included in nanofibers that form non-woven membranes have not been fully studied. It is believed that the surface properties of the nanofibers may promote bacterial adhesion. The porosity of ESF membranes promotes the formation of a biofilm that allows bacterial cells to attach to highly porous

fibers. The rough surface of the nanofibers provides a large area of contact with bacterial cells. Nanofibers with positively charged surfaces facilitate the attachment of negatively charged bacterial cells. The diameter of the fibers (if smaller than the size of the bacteria) can lead to a change in the conformation of the bacterial cells. In addition, hydrophobic bacterial cells adhere to the hydrophobic surfaces of nanofibers due to hydrophobic interactions [105]. Among the materials used to obtain nanofibers with antimicrobial properties by the ESF method is chitosan, a natural polymeric material with insignificant antibacterial activity [106,107]. At the same time, this polymeric material by itself is not capable of completely suppressing the development of pathogenic bacteria [108]. Previously, in the works of our team and colleagues, it was shown that various forms made from PHA itself (microparticles, films, non-woven membranes) do not have an antibacterial effect against gram-negative and gram-positive microorganisms [92,109,110]. Therefore, to impart antibacterial properties to non-woven fibers made from polymers of this family, including the P(3HB-co-4HB) copolymers used in the work, it is necessary to additionally introduce antimicrobial substances into their structure.

The antibacterial activity of non-woven membranes loaded with antibiotics was studied in the culture of opportunistic gram-negative bacteria *E. coli* and gram-positive pathogenic *S. aureus*. The latter is the most common causative agent of skin and soft tissue infections that can cause serious complications [111]. It is believed that gram-positive bacteria are usually more sensitive to the action of antibacterial agents than gram-negative ones, mainly due to differences in the structure and composition of their cell walls [112,113].

It was shown that both types of non-woven membranes loaded with two studied antibiotics have antibacterial activity against both test microorganisms (Figure 6).

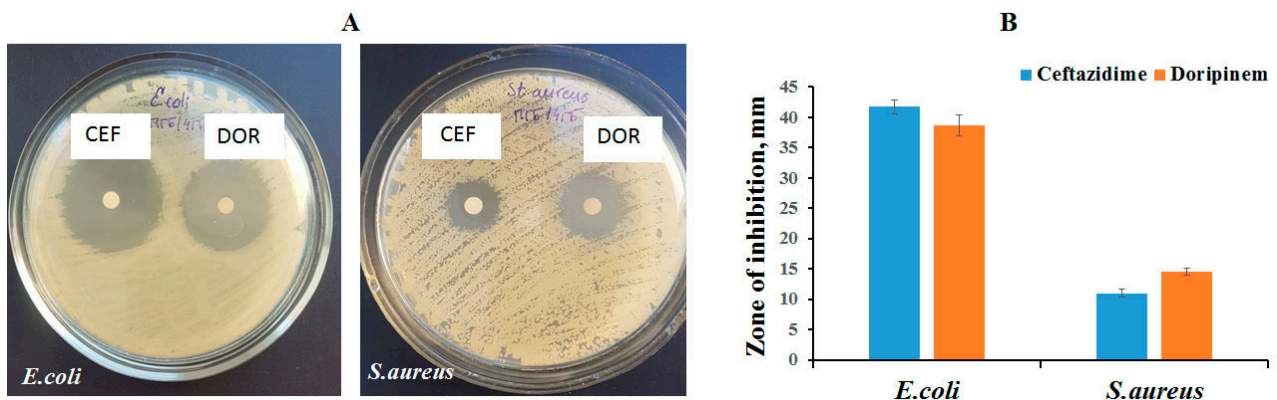


Figure 6. Antimicrobial activity of drug-loaded P(3HB-co-4HB) electrospun nanofibers tested against *E. coli* and *S. aureus*: images of Petri dishes (A) and diameter of zone of inhibition in mm (B). CEF—Ceftazidime, DOR—Doripinem.

E. coli turned out to be a more sensitive microorganism—the diameter of the inhibition zone was 41.7 ± 1.1 and 38.6 ± 1.7 mm when using non-woven membranes containing, respectively, ceftazidime and doripinem. With respect to gram-positive *S. aureus*, the diameter of the zone of inhibition of bacterial growth was on average 3.5 times smaller. At the same time, samples containing doripinem had a more pronounced antibacterial effect. Thus, the diameter of the inhibition zone for the membrane with doripinem was 14.5 ± 0.6 mm.

A similar effect was noted in [63] in the study of non-woven P(3HB) membranes obtained by electrospinning and containing levofloxacin. Gram-positive organisms were more sensitive to the effects of levofloxacin. In addition, the antibacterial effect of fibers with an antibiotic depended on the morphology of the fibers and the content of levofloxacin in them. Another study also showed that non-woven membranes of poly-3-hydroxybutyrate modified with pluronic and containing doxycycline had an antibacterial effect in the culture of *E. coli* and *S. aureus* with zones of inhibition on agar of about 25–30 mm [92]. P(3HB)

non-woven membranes containing kanamycin also inhibited the growth of *S. aureus*; the bacterial growth inhibition zone was 21 mm [64]. In addition, there are examples of PHA non-woven membranes containing various biocides with antibacterial activity in the literature. Kehail et al. [109] obtained samples of non-woven fibers from P(3HB-co-3HHx) copolymer (17 mol.%) with lysozyme immobilized with the enzyme. Non-woven membranes with immobilized lysozyme actively inhibited the growth of *Rhodococcusopacus PD630* when the content of lysozyme in the membrane was 16.1 μg of enzyme per 9.5 mm^3 of membrane. In another work [70], non-woven membranes of the “core-shell” type were obtained from the copolymer P(3HB-co-3HV) (25 mol.%) and polyethylene succinate containing a model biocide, dodecyltrimethylammonium chloride. The antibacterial effect of non-woven membranes with a model biocide was evaluated in a suspension culture of *Pseudomonas aeruginosa*. The authors observed a pronounced decrease in the number of cells in the suspension culture, which reached 98% of the initial number after 4 h from the start of observation.

The results obtained are consistent with the work of colleagues and indicate the promise of using non-woven membranes from biodegradable P(3HB-co-4HB) containing antibiotics to suppress the development of pathogenic microorganisms that infect wound defects of the skin and soft tissues. The manifested prolonged antibacterial effect indicates that the preparations deposited in the nanofibers of non-woven membranes are stable and are not inactivated during electrospinning.

3.4. Evaluation of Biocompatibility of ESF Membranes P(3HB-co-4HB)/Drug in Cell Culture

Non-woven membranes formed by ultrathin nanofibers imitate the extracellular matrix in their structure, providing a natural environment for de novo tissue formation. Compared to other forms of cell carriers, non-woven fibrous membranes promote cell adhesion, proliferation, and differentiation more efficiently due to their high surface to volume ratio [114].

The biological activity of non-woven membranes made of P(3HB-co-4HB) copolymer containing doripinam, ceftazidime, or actovegin was studied in NIH 3T3 mouse fibroblast culture. Figure 7 shows SEM images of fibroblasts on the surface of the samples and fluorescent imaging of nuclei (DAPI stain) and cytoplasm (FITC stain). Differences in the structure of membranes, morphology and diameter of fibers, and their bulk density were reflected in the morphology of adherent and proliferating cells.

In the positive control, on the reference membrane of P3HB-co-4HB without drugs, which has an average fiber diameter of $2.7 \pm 0.5 \mu\text{m}$, the lowest fiber bulk density and the highest value of the contact angle ($123 \pm 5^\circ$), the cells populated the space between the fibers and were weakly flattened, irregularly shaped. The adhesion points were located on one and closely spaced fibers.

Cell nuclei occupied $46 \pm 6\%$ of the non-woven membrane area and had both round and elliptical shapes; the circularity index was 0.7 ± 0.1 . On all samples of non-woven membranes with the inclusion of drugs, with smaller values of the contact angle, regardless of the diameter of the fibers and their bulk density, the cells populated the surfaces of the fibers and were mostly of the correct flat, elongated (spindle-shaped), were well spread and had a greater number of adhesion points on the fibers distant from each other. The area occupied by cell nuclei on non-woven membranes with antibiotics doripinam and ceftazidime was comparable and amounted to 60 ± 3 and 66 ± 5 , respectively. At the same time, on membranes of this type, most nuclei had a spherical shape with a circularity index of 0.8 ± 0.1 . On the non-woven membrane with the inclusion of actovegin, a denser packing of cell nuclei was observed, flattening of the nuclei was noted, and the circularity index was 0.7 ± 0.1 . The number of cells in the control (on reference membranes) was $17.1 \pm 1.0 \times 10^4/\text{cm}^2$. On samples with the antibiotic doripinam, the number of cells was $22.2 \pm 1.2 \times 10^4/\text{cm}^2$; this is 30% higher than the control. A similar number of cells was found on membranes containing ceftazidime ($25.3 \pm 1.4 \times 10^4 \text{ cells}/\text{cm}^2$), which is

50% higher than the control. The maximum number of cells ($29.8 \pm 1.7 \times 10^4/\text{cm}^2$) was registered on the sample with actovegin, i.e., 75% higher than the control.

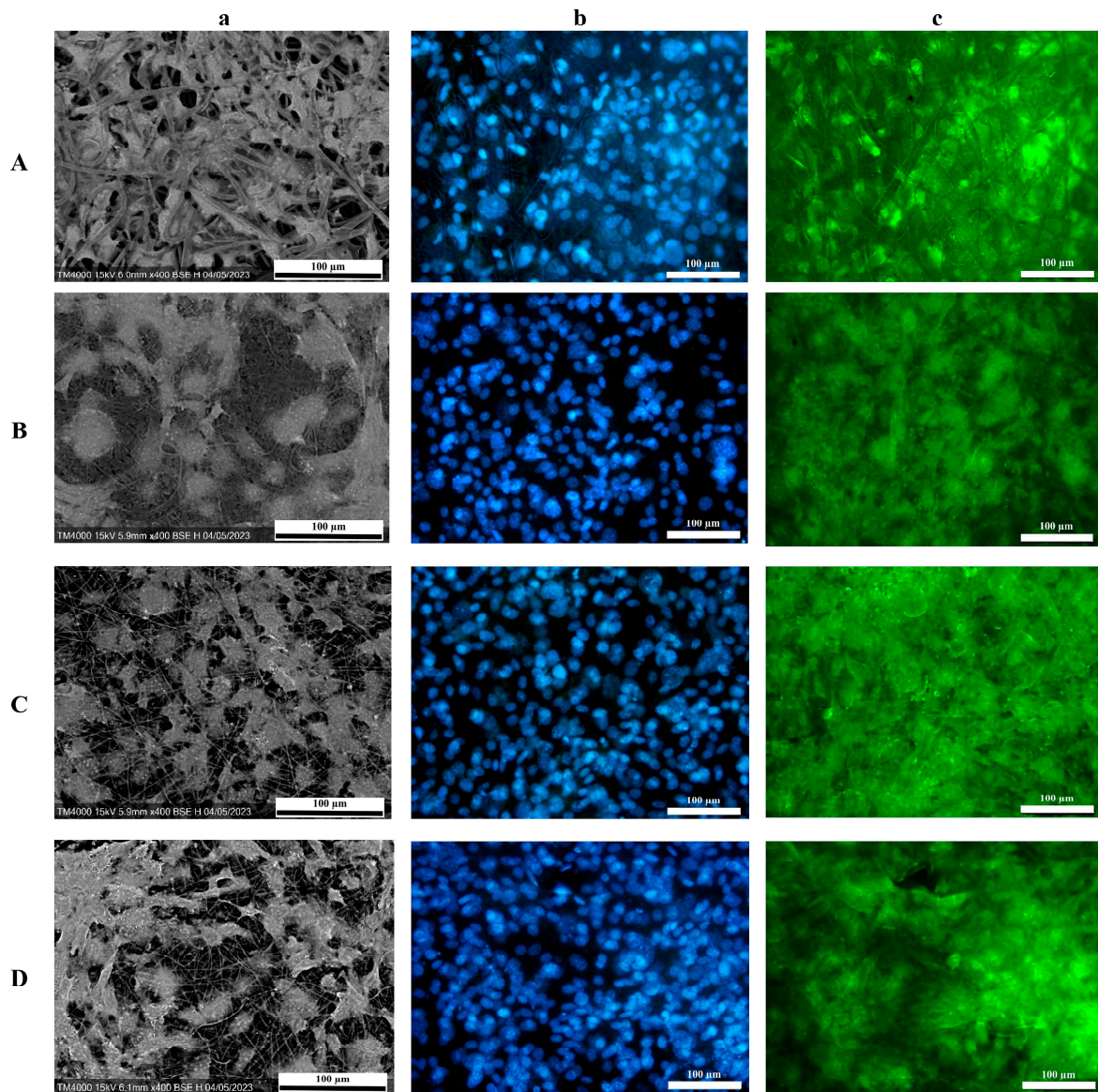


Figure 7. NIH 3T3 fibroblasts cultured on drug-containing P(3HB-co-4HB) non-woven membranes compared to controls (drug-free polymer membranes): A—P(3HB-co-4HB), B—P(3HB-co-4HB)/doripinim, C—P(3HB-co-4HB)/ceftazidime, D—P(3HB-co-4HB)/actovegin. SEM images (a), DAPI (b) and FITC (c) staining. Bar 100 µm.

The results of assessing the viability and metabolic activity of fibroblasts in the MTT test are shown in Figure 8.

The maximum value of cell viability on the 3rd day of cultivation was recorded on membranes containing actovegin, which statistically significantly (at $p < 0.01$) exceeded the values for membranes without drugs. Also, a statistically significant (at the level of $p < 0.05$) increase in the viability and metabolic activity of cells was registered on non-woven membranes with actovegin relative to samples containing doripinim, as well as actovegin. Regardless of the presence of antibiotics, the samples of the studied non-woven membranes did not have a negative effect on cell attachment and proliferation. The indicators of cell viability and metabolic activity were comparable or slightly higher than those on polymer membranes without preparations (positive control), as well as on culture plastic

(negative control). The sample containing actovegin showed little stimulatory effect on NIH 3T3 fibroblasts.

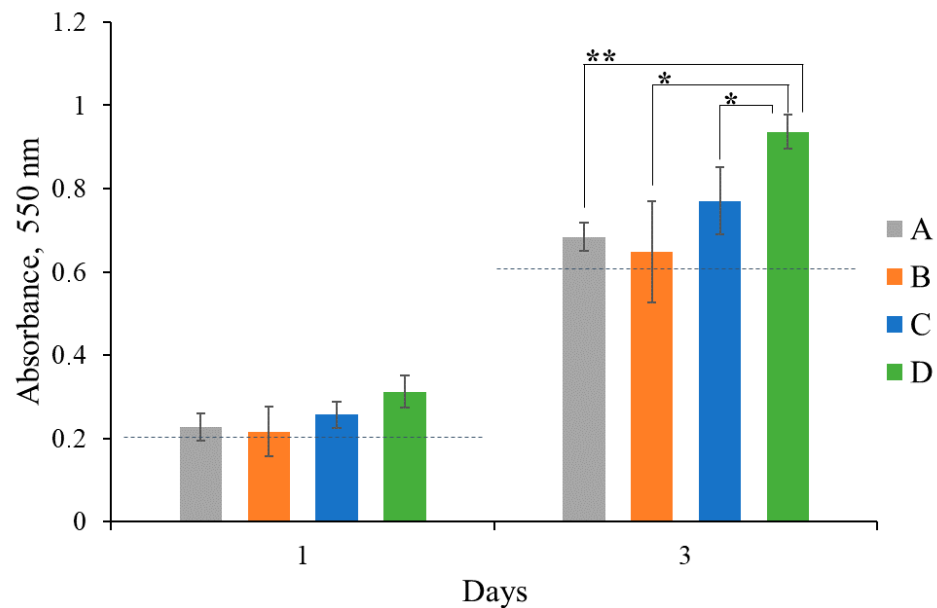


Figure 8. Viability scores of NIH 3T3 fibroblasts cultured on drug-containing P(3HB-co-4HB) non-woven membranes by MTT test versus positive control (polymer membranes without drugs): A—P(3HB-co-4HB), B—P(3HB-co-4HB)/doripinem, C—P(3HB-co-4HB)/ceftazidime, D—P(3HB-co-4HB)/actovegin. The dotted line—indicators on culture plastic (negative control). Data were considered statistically significant at * $p < 0.05$ and ** $p < 0.01$.

The results of evaluating the biological activity of non-woven polymeric membranes containing drugs obtained in the work are consistent with published data. Thus, in [115], gelatin nanofibers obtained by the ESF method with the inclusion of the antioxidant proanthocyanidin in the L-929 mouse fibroblast culture did not show the effect of toxicity, and the presence of proanthocyanidin promoted cell proliferation. A study of the biocompatibility of ESF nanofibers obtained from polylactide and containing the anesthetic drug lidocaine and the antibiotic mupirocin in human fibroblast culture showed that there were significantly more cells of attached cells on the experimental matrices compared to the control. The results indicate that drugs did not inhibit cell proliferation, and such a biosystem would promote wound healing, providing an anesthetic effect [116].

4. Conclusions

Biodegradable microbial copolymers of 3-hydroxybutyrate-co-4-hydroxybutyrate have been used to produce non-woven nanomembranes loaded with drugs using an electrospinning method. The membranes were loaded with antibiotics (ceftazidime and doripinem), and actovegin—a drug that stimulates metabolism, trophism, and tissue regeneration. The influence of the preparation type on the membrane microstructure and fiber sizes was revealed. Membrane loading with drugs reduced the contact angle, increasing the hydrophilicity of the surface. It has been shown that non-woven membranes are a long-term form for the deposition and delivery of drugs. The release of drugs from membranes in vitro was studied and it was shown that it is realized for a long time without sharp releases, and corresponds to the models of Higuchi and Korsmeyer-Peppas. The membranes loaded with antibiotics have antibacterial activity and inhibit the development of *S. aureus* and *E. coli*. In the culture of fibroblasts, it showed no negative effect on cell adhesion and proliferation, despite the presence of antibiotics. The number of viable fibroblasts cultivated on P(3HB-co-4HB)/drug membranes is comparable and/or significantly higher than controls (polymer membranes without drugs and culture plastic. This allows us

to conclude that the developed non-woven membranes are suitable for long-term drug delivery and as carriers for cell technologies, and are promising for the treatment of wound tissue defects during infection.

Author Contributions: T.G.V.—Conceptualization, polymers production; writing—original draft preparation research design, discussion; A.V.D.—investigation, production of ESF membranes; I.N.—SEM studies; A.E.D.—study of surface properties, writing—original draft preparation; A.V.M.—investigation, writing—original draft preparation, study of drug release in vitro; E.I.S.—research in cell cultures, results analysis. All authors have read and agreed to the published version of the manuscript.

Funding: This research was funded by State Assignment of the Ministry of Science and Higher Education of the Russian Federation (project No. 0287-2021-0025).

Institutional Review Board Statement: Not applicable.

Informed Consent Statement: Not applicable.

Data Availability Statement: All data is available in the paper.

Acknowledgments: The authors are especially grateful to the Krasnoyarsk Regional Center for Research Equipment of the Federal Research Center “Krasnoyarsk Scientific Center of the Siberian Branch of the Russian Academy of Sciences” for the equipment provided, and to the Center for Collective Use of the Instrument of the Siberian Federal University for the IR spectra of the samples.

Conflicts of Interest: The authors declare no conflict of interest.

References

1. Gregory, D.A.; Fricker, A.T.R.; Mitrev, P.; Ray, M.; Asare, E.; Sim, D.; Larpmitchai, S.; Zhang, Z.; Ma, J.; Tetali, S.S.V.; et al. Additive Manufacturing of Polyhydroxyalkanoate-Based Blends Using Fused Deposition Modelling for the Development of Biomedical Devices. *J. Funct. Biomater.* **2023**, *14*, 40. [\[CrossRef\]](#)
2. Kalia, V.C.; Patel, S.K.S.; Lee, J.-K. Exploiting Polyhydroxyalkanoates for Biomedical Applications. *Polymers* **2023**, *15*, 1937. [\[CrossRef\]](#)
3. Huang, Z.M.; Zhang, Y.Z.; Kotaki, M.; Ramakrishna, S. A review on polymer nanofibers by electrospinning and their applications in nanocomposites. *Compos. Sci. Technol.* **2003**, *63*, 2223–2253. [\[CrossRef\]](#)
4. Smith, L.A.; Ma, P.X. Nano-fibrous scaffolds for tissue engineering. *Colloids Surf. B Biointerf.* **2004**, *39*, 125–131. [\[CrossRef\]](#) [\[PubMed\]](#)
5. Reneker, D.H.; Kataphinan, W.; Theron, A.; Zussman, E.; Yarin, A.L. Nanofiber garlands of polycaprolactone by electrospinning. *Polymer* **2002**, *43*, 6785–6794. [\[CrossRef\]](#)
6. Yarin, A.L.; Zussman, E. Upward needleless electrospinning of multiple nanofibers. *Polymer* **2004**, *45*, 2977–2980. [\[CrossRef\]](#)
7. Yener, F.; Jirsak, O. Comparison between the Needle and Roller Electrospinning of Polyvinylbutyral. *J. Nanomater.* **2012**, 839317. [\[CrossRef\]](#)
8. Zong, X.; Kim, K.; Fang, D.; Ran, S.; Hsiao, B.S.; Chu, B. Structure and process relationship of electrospun bioabsorbable nanofiber membranes. *Polymer* **2002**, *43*, 4403–4412. [\[CrossRef\]](#)
9. Ding, B.; Wang, M.; Wang, X.; Yu, J.; Sun, G. Electrospun nanomaterials for ultrasensitive sensors. *Mater. Today* **2010**, *13*, 16–27. [\[CrossRef\]](#)
10. Kenawy, E.R.; Layman, J.M.; Watkins, J.R.; Bowlin, G.L.; Matthews, J.A.; Simpson, D.G.; Wnek, G.E. Electrospinning of poly(ethylene-co-vinyl alcohol) fibers. *Biomaterials* **2003**, *24*, 907–913. [\[CrossRef\]](#)
11. Kessing, R.; Fenn, J.; Tepper, G. The use of AC potentials in electrospaying and electrospinning processes. *Polymer* **2004**, *45*, 2981–2984. [\[CrossRef\]](#)
12. Khil, M.S.; Kim, H.K.; Kim, M.S.; Park, S.Y.; Lee, D.R. Nanofibrous mats of poly(trimethylene terephthalate) via electrospinning. *Polymer* **2004**, *45*, 295–301. [\[CrossRef\]](#)
13. Mo, X.M.; Xu, C.Y.; Kotaki, M.; Ramakrishna, S. Electrospun P(LLA-CL) nanofiber: A biomimetic extracellular matrix for smooth muscle cell and endothelial cell proliferation. *Biomaterials* **2004**, *25*, 1883–1890. [\[CrossRef\]](#) [\[PubMed\]](#)
14. Theron, S.A.; Zussman, E.; Yarin, A.L. Experimental investigation of the governing parameters in the electrospinning of polymer solutions. *Polymer* **2004**, *45*, 2017–2030. [\[CrossRef\]](#)
15. Riboldi, S.; Sampaolesi, M.; Neuenschwander, P.; Cossu, G.; Mantero, S. Electrospun degradable polyesterurethane membranes: Potential scaffolds for skeletal muscle tissue. *Biomaterials* **2005**, *26*, 4606–4615. [\[CrossRef\]](#)
16. Hu, S.; Liu, G.; Zhou, Y.; Huang, Z.; Xie, X.; Jing, X. Electrospinning of polymeric nanofibers for drug delivery applications. *J. Control. Release* **2014**, *10*, 12–21. [\[CrossRef\]](#)

17. Kajdič, S.; Planinšek, O.; Gašperlin, M.; Kocbek, P. Electrospun nanofibers for customized drug-delivery systems. *J. Drug Deliv. Sci. Technol.* **2019**, *51*, 672–681. [\[CrossRef\]](#)
18. Akhgari, A.; Shakib, Z.; Sanati, S. A review on electrospun nanofibers for oral drug delivery. *Nanomed. J.* **2017**, *4*, 197–207. [\[CrossRef\]](#)
19. Kajdič, S.; Zupančič, Š.; Roškar, R.; Kocbek, P. The potential of nanofibers to increase solubility and dissolution rate of the poorly soluble and chemically unstable drug lovastatin. *Int. J. Pharm.* **2020**, *573*, 118809. [\[CrossRef\]](#)
20. Carvalho, B.M.; Pellá, M.C.G.; Hardt, J.C.; de Souza Rossin, A.R.; Tonet, A.; Ilipronti, T.; Caetano, J.; Dragunski, D.C. Ecovio[®]-based nanofibers as a potential fast transdermal releaser of aceclofenac. *J. Mol. Liq.* **2021**, *325*, 115206. [\[CrossRef\]](#)
21. Celebioglu, A.; Uyar, T. Electrospun formulation of acyclovir/cyclodextrin nanofibers for fast-dissolving antiviral drug delivery. *Mater. Sci. Eng. C* **2021**, *118*, 111514. [\[CrossRef\]](#)
22. Xu, H.; Zhang, F.; Wang, M.; Lv, H.; Yu, D.G.; Liu, X.; Shen, H. Electrospun hierarchical structural films for effective wound healing. *Biomater. Adv.* **2022**, *136*, 212795. [\[CrossRef\]](#) [\[PubMed\]](#)
23. Jariwala, T.; Ico, G.; Tai, Y.; Park, H.; Myung, N.V.; Nam, J. Mechano-Responsive Piezoelectric Nanofiber as an On-Demand Drug Delivery Vehicle. *ACS Appl. Bio. Mater.* **2021**, *4*, 3706–3715. [\[CrossRef\]](#) [\[PubMed\]](#)
24. Sun, Y.; Cheng, S.; Lu, W.; Wang, Y.; Zhang, P.; Yao, Q. Electrospun fibers and their application in drug controlled release, biological dressings, tissue repair, and enzyme immobilization. *RSC Adv.* **2019**, *9*, 25712–25729. [\[CrossRef\]](#) [\[PubMed\]](#)
25. Abdalkarim, S.Y.H.; Yu, H.; Wang, C.; Chen, Y.; Zou, Z.; Han, L.; Yao, J.; Tamm, K.C. Thermo and light-responsive phase change nanofibers with high energy storage efficiency for energy storage and thermally regulated on-off drug release devices. *Chem. Eng. J.* **2019**, *375*, 121979. [\[CrossRef\]](#)
26. Chen, G.-Q. Plastics Completely Synthesized by Bacteria: Polyhydroxyalkanoates. In *Plastics from Bacteria*; Chen, G.-Q., Ed.; Springer: Berlin/Heidelberg, Germany, 2010; pp. 17–37.
27. Sudesh, K.; Abe, H.; Doi, Y. Synthesis, structure and properties of polyhydroxyalkanoates: Biological polyesters. *Prog. Polym. Sci.* **2000**, *25*, 1503–1555. [\[CrossRef\]](#)
28. Chen, G.-Q.; Jiang, X.-R.; Guo, Y. Synthetic biology of microbes synthesizing polyhydroxyalkanoates (PHA). *Synt. Syst. Biotech.* **2016**, *1*, 236–242. [\[CrossRef\]](#)
29. Koller, M. *The Handbook of Polyhydroxyalkanoates, Postsynthetic Treatment, Processing and Applications*; Taylor & Francis: Oxfordshire, UK, 2020.
30. Koller, M. Polyhydroxyalkanoate biosynthesis at the edge of water activity haloarchaea as biopolyester factories. *Bioengineering* **2019**, *6*, 34. [\[CrossRef\]](#)
31. Koller, M.; Mukherjee, A. Polyhydroxyalkanoates—linking properties, applications, and end-of-life options. *Chem. Biochem. Eng.* **2020**, *34*, 115–129. [\[CrossRef\]](#)
32. Kalia, V.; Gogante, P.; Cinelli, P.; Seggiani, V.A.; Alaverex, A.; Lazzeri, A. Processing and thermomechanical properties of PHA. In *The Handbook of Polyhydroxyalkanoates*; Koller, M., Ed.; Taylor & Francis: Oxfordshire, UK, 2020; pp. 91–118.
33. Lakshmi, S.; Laurencin, C. Biodegradable polymers as biomaterials. *Prog. Polym. Sci.* **2007**, *32*, 762–798. [\[CrossRef\]](#)
34. Philip, S.; Keshavarz, T.; Roy, I. Polyhydroxyalkanoates: Biodegradable polymers with a range of applications. *J. Chem. Technol. Biotechnol.* **2007**, *82*, 233–247. [\[CrossRef\]](#)
35. Kalia, V.; Kumar, S.; Patel, S.; Shanmugam, R.; Lee, J.-K. Polyhydroxyalkanoates: Trends and advances toward biotechnological applications. *Bioresour. Technol.* **2021**, *326*, 124737. [\[CrossRef\]](#) [\[PubMed\]](#)
36. Volova, T.G.; Vinnik, Y.S.; Shishatskaya, E.I.; Markelova, N.M.; Zaikov, G.E. *Natural Based Polymers for Biomedical Applications*; Apple Academic Press: Point Pleasant, NJ, USA, 2017.
37. Zhang, J.; Shishatskaya, E.I.; Volova, T.G.; Ferreira da Silva, L.; Chen, G.Q. Polyhydroxyalkanoates (PHA) for therapeutic applications. *Mater. Sci. Eng. C* **2018**, *86*, 144–150. [\[CrossRef\]](#) [\[PubMed\]](#)
38. Asare, E.; Gregory, D.A.; Frisker, A.; Marcello, E.A.; Paxinou, C.S.; Taylor, J.; Hauck, W.; Roy, I. *Polyhydroxyalkanoates, Their Processing and Biomedical Application*; Koller, M., Ed.; Taylor & Francis: Oxfordshire, UK, 2020; pp. 255–284.
39. Williams, S.F.; Martin, D.P. Applications of polyhydroxyalkanoates (PHA) in medicine and pharmacy. In *Biopolymers*; Steinbüchel, A., Ed.; Wiley-VCH Verlag GmbH & Co. KGaA: Weinheim, Germany, 2005; pp. 91–103. [\[CrossRef\]](#)
40. Chen, G.-Q.; Wu, Q. The application of polyhydroxyalkanoates as tissue engineering materials. *Biomaterials* **2005**, *26*, 6565–6578. [\[CrossRef\]](#)
41. Zhao, X.; Niu, Y.; Mi, C.; Gong, H.; Yang, X.; Cheng, J.; Zhou, Z.; Liu, J.; Peng, X.; Wei, D. Electrospinning nanofibers of microbial polyhydroxyalkanoates for applications in medical tissue engineering. *J. Appl. Polym. Sci.* **2021**, *59*, 1994–2013. [\[CrossRef\]](#)
42. Prakash, P.; Lee, W.-H.; Loo, C.-Y.; Wong, H.S.J.; Parumasivam, T. Advances in Polyhydroxyalkanoate Nanocarriers for Effective Drug Delivery: An Overview and Challenges. *Nanomaterials* **2022**, *12*, 175. [\[CrossRef\]](#)
43. Williams, S.F.; Martin, D.P.; Moses, A.C. The history of GalaFLEX P4HB scaffold. *Aesthetic Surg. J.* **2016**, *36*, 33–42. [\[CrossRef\]](#)
44. Utsunomia, C.; Ren, Q.; Zinn, M. Poly(4-Hydroxybutyrate): Current state and perspectives. *Front. Bioeng. Biotechnol.* **2020**, *8*, 257. [\[CrossRef\]](#)
45. Gordeev, S.A.; Shishatskaya, E.I.; Volova, T.G. Production and study of foreign-oriented poly(hydroxybutyrate/hydroxyvalerate) copolymers. *Perspect. Mater.* **2005**, *3*, 50–55. (In Russian)
46. Gordeev, S.A.; Shishatskaya, E.I.; Volova, T.G. Production of ultrathin fibers from polyhydroxyalkanoates by electrostatic spinning. *Plast. Masses* **2006**, *4*, 49–52. (In Russian)

47. Sombatmankhong, K.; Suwanton, O.; Waleetorncheepsawat, S.; Supaphol, P. Electrospun fiber mats of poly(3-hydroxybutyrate), poly(3-hydroxybutyrate-co-3-hydroxyvalerate), and their blends. *J. Polym. Sci. Part B Polym. Phys.* **2006**, *44*, 2923–2933. [[CrossRef](#)]
48. Cheng, M.L.; Lin, C.C.; Su, H.L.; Chen, P.Y.; Sun, Y.M. Processing and characterization of electrospun poly(3-hydroxybutyrate-co-3-hydroxyhexanoate) nanofibrous membranes. *Polymer* **2008**, *49*, 546–553. [[CrossRef](#)]
49. Wang, Y.; Gao, R.; Wang, P.P.; Jian, J.; Jiang, X.L.; Yan, C.; Lin, X.; Wu, L.; Chen, G.Q.; Wu, Q. The differential effects of aligned electrospun PHBHx fibers on adipogenic and osteogenic potential of MSCs through the regeneration of PPAR signaling. *Biomaterials* **2012**, *3*, 485–493. [[CrossRef](#)]
50. Wang, Z.; Ma, K.; Jiang, X.; Xie, J.; Cai, P.; Li, F.; Liang, R.; Zhao, J.; Zheng, L. Electrospun poly(3-hydroxybutyrate-co-4-hydroxybutyrate)/Octacalcium phosphate Nanofibrous membranes for effective guided bone regeneration. *Mater. Sci. Eng. C* **2020**, *112*, 110763. [[CrossRef](#)] [[PubMed](#)]
51. Wang, P.; Lv, H.; Cao, X.; Liu, Y.; Yu, D. Recent progress of the preparation and application of electrospun porous nanofibers. *Polymers* **2023**, *15*, 921. [[CrossRef](#)] [[PubMed](#)]
52. Volova, T.G.; Goncharov, D.B.; Sukovatyi, A.G.; Shabanov, A.; Nikolaeva, E.D.; Shishatskaya, E.I. Electrospinning of polyhydroxyalkanoate fibrous scaffolds: effect on electrospinning parameters on structure and properties. *J. Biomater. Sci. Polym. Edit.* **2014**, *25*, 370–393. [[CrossRef](#)]
53. Sombatmankhong, K.; Sanchavanakit, N.; Pavasant, P.; Supaphol, P. Bone scaffolds from electrospun fiber mats of poly(3-hydroxybutyrate), poly(3-hydroxybutyrate-co-3-hydroxyvalerate) and their blend. *Polymer* **2007**, *48*, 1419–1427. [[CrossRef](#)]
54. Tong, H.W.; Wang, M. Electrospinning of poly(hydroxybutyrate-co-hydroxyvalerate) fibrous scaffolds for tissue engineering applications: Effects of electrospinning parameters and solution properties. *J. Macromol. Sci.* **2011**, *50*, 1535–1558. [[CrossRef](#)]
55. Tong, H.W.; Wang, M.; Lu, W.L. Electrospinning and evaluation of PHBV-based tissue engineering scaffolds with different fiber diameters, surface topography and compositions. *J. Biomater. Sci.* **2012**, *23*, 779–806. [[CrossRef](#)]
56. Yu, B.Y.; Chen, P.Y.; Sun, Y.M.; Lee, Y.T.; Young, T.H. Response of human mesenchymal stem cells (hmsc) to the topographic variation of poly(3-hydroxybutyrate-co-3-hydroxyhexanoate) (phbhx) films. *J. Biomater. Sci.* **2012**, *23*, 1–26. [[CrossRef](#)]
57. Li, X.T.; Zhang, Y.; Chen, G.Q. Nanofibrous polyhydroxyalkanoates matrices as cell growth supporting materials. *Biomaterials* **2008**, *29*, 3720–3728. [[CrossRef](#)]
58. Bashur, C.A.; Dahlgren, L.A.; Goldstein, A.S. Effect of fiber diameter and orientation on fibroblast morphology and proliferation on electrospun poly(D, L-lactic-co-glycolic acid) meshes. *Biomaterials* **2006**, *27*, 5681–5688. [[CrossRef](#)]
59. Pham, Q.P.; Sharma, U.; Mikos, A.G. Electrospinning of polymeric nanofibers for tissue engineering applications: A review. *Tissue Eng.* **2006**, *12*, 1197–1211. [[CrossRef](#)] [[PubMed](#)]
60. Still, T.J.; von Recum, H.A. Electrospinning: Applications in drug delivery and tissue engineering. *Biomaterials* **2008**, *29*, 1989–2006. [[CrossRef](#)]
61. Lowery, J.L.; Datta, N.G.C. Rutledge, Effect of fiber diameter, pore size and seeding method on growth of human dermal fibroblasts in electrospun poly(ϵ -caprolactone) fibrous mats. *Biomaterials* **2010**, *31*, 491–504. [[CrossRef](#)] [[PubMed](#)]
62. Amini, F.; Semnani, D.; Karbasi, S.; Banitaba, S.N. A novel bilayer drug-loaded wound dressing of PVDF and PHB/Chitosan nanofibers applicable for post-surgical ulcers. *Int. J. Polym. Mater.* **2018**, *68*, 772–777. [[CrossRef](#)]
63. Kundrat, V.; Cernekova, N.; Kovalcik, A.; Enev, V.; Marova, I. Drug Release Kinetics of Electrospun PHB Meshes. *Materials* **2019**, *12*, 1924. [[CrossRef](#)]
64. Naveen, N.; Kumar, R.; Balaji, S.; Uma, T.; Natrajan, T.; Sehgal, P. Synthesis of Nonwoven Nanofibers by Electrospinning—A Promising Biomaterial for Tissue Engineering and Drug Delivery. *Adv. Eng. Mater.* **2010**, *12*, B380–B387. [[CrossRef](#)]
65. Mukheem, A.; Muthoosamy, K.; Manickam, S.; Sudesh, K.; Shahabuddin, S.; Saidur, R.; Akbar, N.; Sridewi, N. Fabrication and Characterization of an Electrospun PHA/Graphene Silver Nanocomposite Scaffold for Antibacterial Applications. *Materials* **2018**, *11*, 1673. [[CrossRef](#)]
66. Mukheem, A.; Shahabuddin, S.; Akbar, N.; Miskon, A.; Sarih, N.M.; Sudesh, K.; Khan, N.A.; Saidur, R.; Sridewi, N. Boron Nitride Doped Polyhydroxyalkanoate/Chitosan Nanocomposite for Antibacterial and Biological Applications. *Nanomaterials* **2019**, *9*, 645. [[CrossRef](#)]
67. Xing, Z.C.; Chae, W.P.; Baek, J.Y.; Choi, M.J.; Jung, Y.; Kang, I.K. In Vitro Assessment of Antibacterial Activity and Cytocompatibility of Silver-Containing PHBV Nanofibrous Scaffolds for Tissue Engineering. *Biomacromolecules* **2010**, *11*, 1248–1253. [[CrossRef](#)]
68. Douglass, M.; Hopkins, S.; Pandey, R.; Singha, P.; Norman, M.; Handa, H. S-Nitrosoglutathione-Based Nitric Oxide-Releasing Nanofibers Exhibit Dual Antimicrobial and Antithrombotic Activity for Biomedical Applications. *Macromol. Biosci.* **2021**, *21*, 2000248. [[CrossRef](#)]
69. Shiny, P.J.; Devi, M.V.; Grace Felciya, S.J.; Ramanathan, G.; Fardim, P.; Sivagnanam, U.T. In vitro and in vivo evaluation of poly-3-hydroxybutyric acid-sodium alginate as a core-shell nanofibrous matrix with arginine and bacitracin-nanoclay complex for dermal reconstruction of excision wound. *Int. Biol. Macromol.* **2021**, *168*, 46–58. [[CrossRef](#)] [[PubMed](#)]
70. Li, W.; Cicek, N.; Levin, D.B.; Logsetty, S.; Liu, S. Bacteria-triggered release of a potent biocide from core-shell polyhydroxyalkanoate (PHA)-based nanofibers for wound dressing applications. *J. Biomater. Sci. Polym. Ed.* **2020**, *31*, 394–406. [[CrossRef](#)]
71. Volova, T.; Shishatskaya, E. Bacterial Strain VKPM B-10646—A Producer of Polyhydroxyalkanoates and a Method of Their Production). RF Patent No. 2439143, 10 January 2012.

72. Volova, T.; Kiselev, E.; Nemtsev, I.; Lukyanenko, A.; Sukovatyi, A.; Kuzmin, A.; Ryltseva, G.; Shishatskaya, E. Properties of Degradable Polyhydroxyalkanoates with Different Monomer Compositions. *Int. J. Biol. Macromol.* **2021**, *182*, 98–114. [[CrossRef](#)] [[PubMed](#)]
73. Kaelble, D.H. Dispersion-Polar Surface Tension Properties of Organic Solids. *J. Adhes.* **1970**, *2*, 66–81. [[CrossRef](#)]
74. Owens, D.K.; Wendt, R.C. Estimation of the Surface Free Energy of Polymers. *J. Appl. Polym. Sci.* **1969**, *13*, 1741–1747. [[CrossRef](#)]
75. Dash, S.; Murthy, P.N.; Nath, L.; Chowdhury, P. Kinetic Modeling on Drug Release from Controlled Drug Delivery Systems. *Acta Pol. Pharm.* **2010**, *67*, 217–223.
76. Fu, Y.; Kao, W.J. Drug Release Kinetics and Transport Mechanisms of Non-Degradable and Degradable Polymeric Delivery Systems. *Expert Opin. Drug Deliv.* **2010**, *7*, 429–444. [[CrossRef](#)]
77. Cavalieri, S.J. *Manual of Antimicrobial Susceptibility Testing*; American Society for Microbiology: Washington, DC, USA, 2009; p. 241.
78. Martin, D.P.; Williams, S.F. Medical applications of poly-4-hydroxybutyrate: A strong flexible absorbable biomaterial. *Biochem. Eng. J.* **2003**, *16*, 97–105. [[CrossRef](#)]
79. de Macedo, M.A.; Oliveira Filho, E.R.; Taciro, M.K.; Piccoli, R.A.M.; Gomez, J.G.C.; Silva, L.F. Poly(3 hydroxybutyrate co 4 hydroxybutyrate) [P(3HB co 4HB)] biotechnological production: Challenges and opportunities. *Biomass Convers. Biorefinery* **2022**. [[CrossRef](#)]
80. Nelson, T.; Kaufman, E.; Kline, J.; Sokoloff, L. The extraneural distribution of g-hydroxybutyrate. *J. Neurochem.* **1981**, *37*, 1345–1348. [[CrossRef](#)] [[PubMed](#)]
81. Sendelbeck, S.L.; Girdis, C.L. Disposition of a ¹⁴C-labeled bioerodible polyorthoester and its hydrolysis products, 4-hydroxybutyrate and cis, trans-1,4-bis(hydroxymethyl) cyclohexane, in rats. *Drug Metab. Dispos.* **1985**, *13*, 291–295.
82. Lide, D.R. *Handbook of Chemistry and Physics*, 86th ed.; CRC; Taylor & Francis: Boca Raton, FL, USA, 2005.
83. Serjeant, E.P.; Dempsey, B. *Ionisation Constants of Organic acids in Aqueous Solution*; Pergamon Press: New York, NY, USA, 1979.
84. O'Neil, M.J. *The Merck Index: An Encyclopedia of Chemicals, Drugs, and Biologicals*; RSC Publishing: Cambridge, UK, 2013.
85. Volova, T.G.; Prudnikova, S.V.; Vinogradova, O.N.; Syrvacheva, D.A.; Shishatskaya, E.I. A study of microorganisms degrading PHAs with different chemical compositions and PHA biodegradation behavior. *Microb. Ecol.* **2017**, *73*, 353–367. [[CrossRef](#)] [[PubMed](#)]
86. Hu, J.; Prabhakaran, M.P.; Tian, L.L.; Ding, X.; Ramakrishna, S. Drug-loaded emulsion electrospun nanofibers: Characterization, drug release and in vitro biocompatibility. *RSC Adv.* **2015**, *5*, 100256–100267. [[CrossRef](#)]
87. Wang, W.; Cao, J.D.; Lan, P.; Wu, W. Drug release from electrospun fibers of poly (3-hydroxybutyrate-co-3-hydroxyvalerate) grafted with poly (N-vinylpyrrolidone). *J. Appl. Polym. Sci.* **2012**, *124*, 1919–1928. [[CrossRef](#)]
88. Kaniuk, L.; Stachewicz, U. Development and Advantages of Biodegradable PHA Polymers Based on Electrospun PHBV Fibers for Tissue Engineering and Other Biomedical Applications. *ACS Biomater. Sci. Eng.* **2021**, *7*, 5339–5362. [[CrossRef](#)]
89. Sanhueza, C.; Acevedo, F.; Rocha, S.; Villegas, P.; Seeger, M.; Navia, R. Polyhydroxyalkanoates as Biomaterial for Electrospun Scaffolds. *Int. J. Biol. Macromol.* **2019**, *124*, 102–110. [[CrossRef](#)]
90. Ding, J.; Zhang, J.; Li, J.; Li, D.; Xiao, C.; Xiao, H.; Yang, H.; Zhuang, X.; Chen, X. Electrospun Polymer Biomaterials. *Prog. Polym. Sci.* **2019**, *90*, 1–34. [[CrossRef](#)]
91. Chen, Y.; Abdalkarima, S.Y.; Yu, H.Y.; Li, Y.; Xu, J.; Marek, J.; Yao, J.; Tam, K. Double stimuli-responsive cellulose nanocrystals reinforced electrospun PHBV composites membrane for intelligent drug release. *Inter. J. Biol. Macromol.* **2020**, *155*, 330–339. [[CrossRef](#)]
92. Bhattacharjee, A.; Kumar, K.; Arora, A.; Katti, D.S. Fabrication and characterization of Pluronic modified poly(hydroxybutyrate) fibers for potential wound dressing applications. *Mater. Sci. Engin. C* **2016**, *63*, 266–273. [[CrossRef](#)] [[PubMed](#)]
93. Ang, S.L.; Shaharuddin, B.; Chuah, J.A.; Sudesh, K. Electrospun poly(3-hydroxybutyrate-co-3-hydroxyhexanoate)/silk fibroin film is a promising scaffold for bone tissue engineering. *Inter. J. Biol. Macromol.* **2020**, *145*, 173–188. [[CrossRef](#)] [[PubMed](#)]
94. Safdari, M.; Shakiba, E.; Kiaie, S.; Fattahi, A. Preparation and characterization of ceftazidime loaded electrospun silk fibroin/gelatin mat for wound dressing. *Fibers Polym.* **2016**, *17*, 744–750. [[CrossRef](#)]
95. Mendez, A.; Mantovani, L.; Barbosa, F.; Sayago, C.T.M.; Garcia, C.V.; Paula, F.R.; Denardin, F. Characterization of the antibiotic doripinem using physicochemical methods—chromatography, spectrophotometry, spectroscopy and thermal analysis. *Quim. Nova* **2011**, *34*, 1634–1638. [[CrossRef](#)]
96. Lee, Y.F.; Sridewi, N.; Ramanathan, S.; Sudesh, K. The Influence of Electrospinning Parameters and Drug Loading on Polyhydroxyalkanoate (PHA) Nanofibers for Drug Delivery. *Inter. J. Biotech. Wellness Ind.* **2015**, *4*, 103–113. [[CrossRef](#)]
97. Jiffrin, R.; Razak, S.I.; Jamaludin, M.I.; Hamzah, A.S.; Mazian, M.A.; Jaya, M.A.; Nasrullah, M.Z.; Majrashi, M.; Theyab, A.; Aldarmahi, A.A.; et al. Electrospun Nanofiber Composites for Drug Delivery: A Review on Current Progresses. *Polymers* **2022**, *14*, 3725. [[CrossRef](#)] [[PubMed](#)]
98. Anderson, A.J.; Dawes, E.A. Occurrence, metabolism, metabolic role, and industrial uses of bacterial polyhydroxyalkanoates. *Microbiol. Rev.* **1990**, *54*, 450–472. [[CrossRef](#)] [[PubMed](#)]
99. Ong, S.; Chee, J.Y.; Sudesh, K. Degradation of polyhydroxyalkanoate (PHA): A review. *J. Sib. Fed. Univ. Biol.* **2017**, *10*, 211–225. [[CrossRef](#)]
100. Cheng, G.; Cai, Z.; Wang, L. Biocompatibility and biodegradation of poly(hydroxybutyrate)/ poly(ethylene glycol) blend films. *J. Mater. Sci. Mater. Med.* **2003**, *14*, 1073–1078. [[CrossRef](#)]

101. Freier, T.; Kunze, C.; Nischan, C.; Kramer, S.; Sternberg, K.; Hoptu, T.; Schmitz, K.P. In vitro and in vivo degradation studies for development of a biodegradable patch based on poly(3-hydroxybutyrate). *Biomaterials* **2002**, *23*, 2649–2657. [[CrossRef](#)]
102. Machicao, F.; Muresanu, D.F.; Hundesberger, H.; Pflüger, M.; Guekht, A. Pleiotropic neuroprotective and metabolic effects of actovegin. *Neuromuscul. Dis.* **2012**, *4*, 28–35. (In Russia)
103. Drug Database Online. Available online: <https://go.drugbank.com/> (accessed on 20 January 2023).
104. Peppas, N.A.; Narasimhan, B. Mathematical models in drug delivery: How modeling has shaped the way we design new drug delivery systems. *J. Control. Release* **2014**, *190*, 75–81. [[CrossRef](#)] [[PubMed](#)]
105. Ladhari, S.; Vu, N.N.; Boisvert, C.; Saidi, A.; Nguyen-Tri, P. Recent Development of Polyhydroxyalkanoates (PHA)-Based Materials for Antibacterial Applications: A Review. *ACS Appl. Bio Mater.* **2023**, *6*, 1398–1430. [[CrossRef](#)] [[PubMed](#)]
106. Arkoun, M.; Daigle, F.; Heuzey, M.C.; Aji, A. Mechanism of Action of Electrospun Chitosan-Based Nanofibers against Meat Spoilage and Pathogenic Bacteria. *Molecules* **2017**, *22*, 585. [[CrossRef](#)] [[PubMed](#)]
107. Abadi, M.S.S.; Mirzaei, E.; Bazargani, A.; Gholipour, A.; Heidari, H.; Hadi, N. Antibacterial activity and mechanism of action of chitosan nanofibers against toxigenic Clostridioides (Clostridium) difficile Isolates. *Ann. Ig.* **2020**, *32*, 72–80. [[CrossRef](#)]
108. Hamdan, N.; Yamin, A.; Hamid, S.A.; Khodir, W.K.; Guarino, V. Functionalized Antimicrobial Nanofibers: Design Criteria and Recent Advances. *J. Funct. Biomater.* **2021**, *12*, 59. [[CrossRef](#)]
109. Kehail, A.; Brigham, C.J. Anti-biofilm Activity of Solvent-Cast and Electrospun Polyhydroxyalkanoate Membranes Treated with Lysozyme. *J. Polym. Environ.* **2018**, *26*, 66–72. [[CrossRef](#)]
110. Murueva, A.V.; Shershneva, A.M.; Abanina, K.V.; Prudnikova, S.V.; Shishatskaya, E.I. Development and characterization of ceftriaxone-loaded P3HB-based microparticles for drug delivery. *J. Drying Tech.* **2019**, *37*, 1131–1142. [[CrossRef](#)]
111. Giacometti, A.; Cirioni, O.; Schimizzi, A.M.; Del Prete, M.S.; Barchiesi, F.; D’Errico, M.M.; Petrelli, E.; Scalise, G. Epidemiology and microbiology of surgical wound infections. *J. Clin. Microbiol.* **2000**, *38*, 918–922. [[CrossRef](#)]
112. Soares, G.M.S.; Figueiredo, L.C.; Faveri, M.; Cortelli, S.C.; Duarte, P.M.; Feres, M. Mechanisms of action of systemic antibiotics used in periodontal treatment and mechanisms of bacterial resistance to these drugs. *J. Appl. Oral Sci.* **2012**, *20*, 295–309. [[CrossRef](#)]
113. Kapoor, G.; Saigal, S.; Elongavan, A. Action and resistance mechanisms of antibiotics: A guide for clinicians. *J. Anaesthesiol. Clin. Pharmacol.* **2017**, *33*, 300–305. [[CrossRef](#)] [[PubMed](#)]
114. Hutmacher, D.W. Scaffold design and fabrication technologies for engineering tissues—state of the art and future perspectives. *J. Biomater. Sci. Polym. Ed.* **2001**, *12*, 107–124. [[CrossRef](#)] [[PubMed](#)]
115. Huang, C.H.; Chi, C.Y.; Chen, Y.-S.; Chen, K.-Y.; Chen, P.-L.; Yao, C.-H. Evaluation of proanthocyanidin-crosslinked electrospun gelatin nanofibers for drug delivering system. *Mater. Sci. Engin. C* **2012**, *32*, 2476–2483. [[CrossRef](#)]
116. Thakur, R.A.; Florek, C.A.; Kohn, J.; Michniak, B.B. Electrospun nanofibrous polymeric scaffold with targeted drug release profiles for potential application as wound dressing. *Inter. J. of Pharm.* **2008**, *364*, 87–93. [[CrossRef](#)] [[PubMed](#)]

Disclaimer/Publisher’s Note: The statements, opinions and data contained in all publications are solely those of the individual author(s) and contributor(s) and not of MDPI and/or the editor(s). MDPI and/or the editor(s) disclaim responsibility for any injury to people or property resulting from any ideas, methods, instructions or products referred to in the content.